ELISA kit (Pierce Biotechnology Rockford, IL) according to the manufacturer's instructions.

Inhibitory effect of canolol on activation of macrophages from the BALB/c mouse

Macrophages were obtained from the peritoneal fluid of mice stimulated with casein. In brief, 1 ml of 5% casein sodium (Wako Pure Chemical) in phosphate-buffered saline was injected intraperitoneally into BALB/c mice. After 3 days, mice were killed, and 5 ml of cold phosphate-buffered saline was injected into the peritoneal cavity, after which peritoneal lavage fluid (~5 ml) was collected, followed by centrifugation of the fluid (1000 r.p.m., 5 min) at 4°C. The macrophages were washed with phosphate-buffered saline three times by centrifugation, and then 15 ml of Roswell Park Memorial Institute 1640 medium (Invitrogen) with 10% FBS was added and macrophages were cultured in a plastic petri dish (100×26 mm; Nunc A/S, Roskilde, Denmark).

To activate the macrophages in culture, lipopolysaccharide (LPS) (1.0 μg/ml) and interferon-γ (0.1 μg/ml) (Sigma) were added to the cells for 24 h. Culture medium was then collected for measurement of the concentration of nitrite, which is formed from nitric oxide (NO). A significantly high amount of NO was generated by activated macrophages, which was attributable to the action of inducible NO synthase (iNOS). The nitrite concentration was quantified by using a Griess reagent kit (NO_2/NO_3 Assay Kit-C II; Dojindo Laboratories), according to the manufacturer's instructions. The production of inflammatory cytokines, i.e. TNF-α and IL-12, was also measured in culture media by using ELISA as mentioned above.

Protective effect of canolol against $ONOO^-$-induced cytotoxicity

HEK293 cells were plated at 3000 cells/well in a 96-well plate (Nunc A/S). After overnight preincubation, 1 mM or 2 mM 3-(4-morpholinyl)sydnonimine hydrochloride [SIN-1 (Dojindo Laboratories)], from which $ONOO^-$ was produced, was added to the cells. Canolol at various concentrations was then added. After an additional 48 h of incubation, cell viability was determined by using the 3-(4,5-dimethyl-2-thiazolyl)-2,5-diphenyl-2H-tetrazolium bromide (MTT) assay.

Expression of COX-2, TNF-α, iNOS and heme oxygenase-1 in colon tissues of AOM/DSS-induced carcinogenesis mice with/without feeding canolol

To examine the antioxidative, anti-inflammatory mechanisms of canolol in chemoprevention against AOM/DSS-induced colon carcinogenesis, mRNA expressions of representative oxidative inflammatory molecules [i.e. COX-2, TNF-α, heme oxygenase-1 (HO-1) and iNOS] were detected by reverse transcription–polymerase chain reaction. Briefly, after the protocol of AOM/DSS-induced carcinogenesis, total RNA from colon tissues of distal quarter in which most tumors were observed was extracted by using Sepasol®-RNA I Super reagent (NACALAI TESQUE, Kyoto, Japan), according to the manufacturer's instruction. The nucleotide sequences of the oligonucleotide primers and cycle conditions of PCR are as follows: COX-2: forward, 5′-ACA CAC TCT ATC ACT GGC ACC-3′; reverse, 5′-TTC AGG GAG AAG CGT TTG C-3′; 35 cycles of 15 s at 94°C, 15 s at 55°C and 1 min at 72°C to obtain a 274-bp cDNA; TNF-α: forward, 5′-CTA TGT CTC AGC CTC TTC TC-3′; reverse, 5′- CAG CCT TGT CCC TTG AAG AG -3′; 40 cycles of 15 s at 94°C, 30 s at 56°C and 30 s at 68°C to obtain a 353-bp cDNA; HO-1: forward, 5′-GGC CCT GGA AGA GGA GAT AG-3′; reverse, 5′-GCT GGA TGT GCT TTT GGT G-3′; 30 cycles of 30 s at 94°C, 30 s at 56°C and 30 s at 72°C to obtain a 888-bp cDNA; iNOS: forward, 5′-CCC TTC CGA AGT TTC TGG CAG CAG C-3′; reverse, 5′-GGC TGT CAG AGC CTC GTG GCT TTG G-3′; 35 cycles of 1 min at 95°C, 1 min at 65°C and 2 min at 72°C to obtain a 496-bp cDNA; GAPDH (inner control): forward, 5′-CAT GTG GGC CAT GAG GTC CAC CAC-3′; reverse, 5′-TGA AGG TCG GAG TCA ACG GAT TTG GT-3′; 30 cycles of 1 min at 94°C, 1 min at 56°C and 1 min at 72°C to obtain a 983-bp cDNA. PCR products then underwent electrophoresis on ethidium bromide-stained 1.2% agarose gels.

Safety of canolol

Female ICR mice, beginning 6 weeks of age, were fed normal diet (untreated control) or 0.3% canolol for 6 weeks. Then, mice were killed, and blood samples were obtained. Red blood cell count, white blood cell count and hemoglobin levels were determined using an automated blood counter (F-800 Microcell Counter, Toa Medical Electronics, Kobe, Japan). Plasma obtained by centrifugation was used for measurement of the liver and the kidney functions including alanine aminotransferase, aspartate aminotransferase, lactate dehydrogenase, blood urea nitrogen and total creatine using a sequential multiple Auto Analyzer system (Hitachi Ltd., Tokyo, Japan).

Statistical analyses

Data were analyzed by one-way analysis of variance followed by the Bonferroni *t*-test. Some studies with two experiments were analyzed by Mann–Whitney *U*-test, and a Fisher's exact test was used to analyze the data of tumor incidence. A difference was considered statistically significant when $P < 0.05$.

Results

Protective effect of canolol against DSS-induced colitis

Severe diarrhea accompanied by hematochezia, characterized by significant increase in DAI, was observed on day 7 in the DSS-induced colitis group without canolol; these DSS-treated mice showed a decrease in body weight though no statistical significance was found (Table I). These symptoms were markedly improved with significantly decreased DAI when canolol was added to the diet in a dose-dependent manner, and these mice showed no apparent loss of body weight (Table I). Moreover, mice with DSS-induced colitis demonstrated shortening of the large bowel, which is one of the indexes of colitis, and this pathological change was significantly improved by canolol dose dependently (Table I). No significant differences in DAI and in length of large bowel were observed in mice receiving 1% of canolol compared with normal mice (Table I), suggesting an almost complete cure of colitis. However, 1% of canolol becomes impracticable as a chemopreventive agent or supplement especially for long-term application, i.e. canolol

Table I. Protective effect of canolol against DSS-induced colitis (on day 7) and AOM/DSS-induced colon carcinogenesis (at 6 weeks)

Group	Body weight (g)	Liver weight (g)	Length of large bowel (cm)	DAI[a]
Normal	29.7±2.0	3.1±0.7	15.0±1.5**	0
DSS	26.9±4.4	2.4±0.6	9.6±2.1	9.6±0.3
DSS + 0.1% canolol	27.6±2.2	2.8±0.5	12.8±1.2*	5.2±0.7**
DSS + 0.3% canolol	28.8±3.3	2.7±0.5	13.3±2.1**#	3.7±0.6**
DSS + 1% canolol	29.3±1.5	2.9±0.1	13.7±1.7**#	1.2±1.8**#

Group	Body weight (g)	Liver weight (g)	Length of large bowel (cm)[#]	Incidence and multiplicity of tumors	
				Tumor incidence (%)[b]	Tumor multiplicity (no. of tumors/animal)
Normal	48.0±4.7	2.5±0.4	13.0±0.9**	0**	0
AOM/DSS	44.0±3.3	2.0±0.2	8.7±0.6	100	10.8±4.2
AOM/DSS + 0.1% canolol	44.6±6.1	2.1±0.1	10.9±0.9*	60**	5.3±2.7*
AOM/DSS + 0.3% canolol	44.7±1.9	2.0±0.1	10.7±0.3*	57**	5.6±2.7*

Data are means ± SD, $n = 5$–14 for DSS-induced colitis experiments, and $n = 10$–20 for AOM/DSS-induced colon carcinogenesis experiments.
[a]See text for details.
[b]Statistical significance was analyzed by Fisher's exact test.
*$P < 0.05$, **$P < 0.01$, versus the DSS control group, or versus the AOM/DSS control group.
#No significant difference ($P > 0.05$), versus normal group.

needs to be given more than 10 g a day in humans. Canolol at higher than 0.3% was not pursued in the carcinogenesis study and was not subjected for further investigations, i.e. pathological studies and examination of inflammatory cytokines.

Regarding the histopathology of the colon, as Figure 1 shows, the canolol-treated groups (Figure 1C and D) had much less tissue damage compared with the DSS control (Figure 1B) showing severe inflammation and erosion. Inflammation looks more alleviated in the higher dose (0.3%) group (Figure 1D) resembling normal mucosa (Figure 1A) than in the lower dose (0.1%) group (Figure 1C). After 7 days of consumption of the canolol diet, mice in both canolol groups showed significantly suppressed formation of ulcers in the colonic mucosa compared with the DSS-induced colitis group without canolol (Figure 1E).

Canolol exhibits anti-inflammatory and antioxidative activity in DSS-induced colitis

COX-2-specific immunostaining confirmed that DSS-induced colitis clearly associated with colon inflammation (Figure 2A). The COX-2 expressions in DSS control mice were significantly higher than that in normal ICR mice. However, we found the scores of COX-2 in the canolol-treated groups were reduced compared with the DSS control, though no significance was observed ($P = 0.063$).

Consistent with these findings, amount of free 8-OHdG in the plasma, that is a common index for oxidative injury of DNA, was significantly increased after DSS treatment, whereas it was suppressed dose dependently by canolol; a significant difference was observed between DSS group and DSS + 0.3% canolol group (Figure 2B).

Suppression of inflammatory cytokine production in vivo *by canolol treatment in the DSS-induced colitis model*

The anti-inflammatory tissue protective effect of canolol was further confirmed by measuring the IL-12 and TNF-α levels, which are major cytokines involved in cell killing, in the serum of mice with DSS-induced colitis. As seen in Figure 2C and D, DSS-treated mice had significantly elevated levels of both cytokines, whereas these levels decreased after treatment with canolol in a dose-dependent manner, though no significance was observed for 0.1% canolol group compared with DSS control group. This finding is consistent with the improved symptoms and pathology of colitis as noted in Table I.

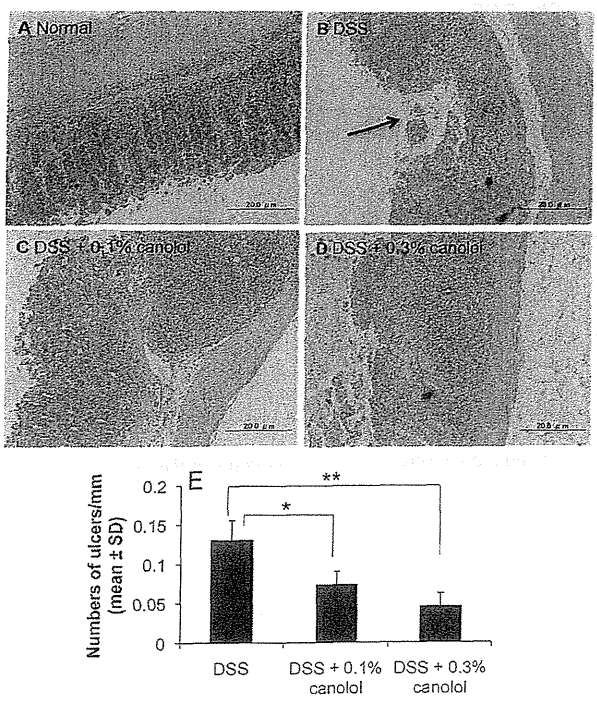

Fig. 1. Histological examination of the large bowel in DSS-induced colitis, with and without canolol treatment. (**A–D**) Hematoxylin and eosin staining of colon tissue from each experimental group. The arrow indicates the ulcer (necrosis) in the colonic mucosa. (**E**) Quantification and summary of the numbers of ulcers in each experimental group. See text for details. Data are means ± SD; $n = 6$–10. $^*P < 0.05$, $^{**}P < 0.01$.

Suppression of macrophage activation and cytokine production by canolol in vitro

The effect of canolol on the progression of inflammation as manifested by macrophage activation was investigated *in vitro* with macrophages from BALB/c mice. Canolol, at concentrations up to 200 μM, showed no apparent cytotoxicity in macrophages and human colon cancer Caco-2 cells (Supplementary Figure 2A and B, available at *Carcinogenesis* Online). Activation of macrophages was induced by simultaneously adding LPS and interferon-γ, and activation was assessed by measuring the generation of NO as nitrite (Figure 3A). Under the same conditions, when canolol was added to the cells, macrophage activation was significantly inhibited in a dose-dependent manner (Figure 3A). Moreover, canolol treatment significantly suppressed generation of inflammatory cytokines (i.e. IL-12 and TNF-α) by the macrophages (Figure 3B and C). These data clearly indicate the anti-inflammatory effect of canolol.

Protective effect of canolol against $ONOO^-$-induced cytotoxicity

Canolol is known as a compound with potent antioxidative activity, which is thought to contribute to its anti-inflammatory and cancer-preventive effects. To evaluate this, we investigated the cytoprotective effect of canolol against $ONOO^-$, which is highly cytotoxic to many cells including bacteria (14,15,20,21). $ONOO^-$ is an endogenous product of NO plus superoxide anion radical (O_2^-) in inflammatory reactions (22), and it can damage DNA, RNA, proteins and other critical molecules by means of oxidation, nitration and hydroxylation (23,24). To investigate the cytotoxicity of $ONOO^-$ and the antioxidative cytoprotection of canolol, we selected a normal cell line, human embryonic kidney cells HEK293. In this *in vitro* system, we found that ~50–60% of cells died after treatment with $ONOO^-$, which was supplied by means of a donor, SIN-1, at 1 mM (Figure 3D). Because of the short half-lives of SIN-1 (1–2 h in plasma) and $ONOO^-$ (2–3 s at physiological pH), the cytotoxicity of $ONOO^-$ in this *in vitro* culture study may be underestimated. However, the important finding is the significant inhibition of $ONOO^-$-induced cytotoxicity by canolol. In addition, a dose-dependent effect of canolol observed in HEK293 cells and the cytotoxicity of 1 mM SIN-1 was completely inhibited by 50 μM canolol (Figure 3D). In addition, canolol itself had no apparent cytotoxicity for this cell line, at least up to 100 μM (Supplementary Figure 2C, available at *Carcinogenesis* Online), which suggests that canolol is safe.

Preventive effect of canolol on AOM/DSS-induced colon carcinogenesis

Inflammatory colitis is believed to be closely associated with the occurrence of colon cancer (1–4). We, thus, investigated the preventive effect of canolol in the AOM/DSS-induced colon carcinogenesis model. The results, as shown in Table I, clearly indicated the suppressive effect of canolol on the occurrence of colon cancer. Compared with AOM/DSS control mice, 100% of which had colon tumors, ~40% of canolol-treated mice did not have these tumors. In addition, the multiplicity was significantly reduced by ~50% in the canolol-treated group compared with the untreated control group (Table I). This effect showed no clear dose dependence, as 0.1 and 0.3% canolol produced similar effect.

Suppression of COX-2, TNF-α, iNOS and HO-1 expression by canolol in AOM/DSS-induced colon carcinogenesis

To investigate the chemopreventive mechanisms of canolol, we measured mRNA expression of proinflammatory cytokines, i.e. COX-2,

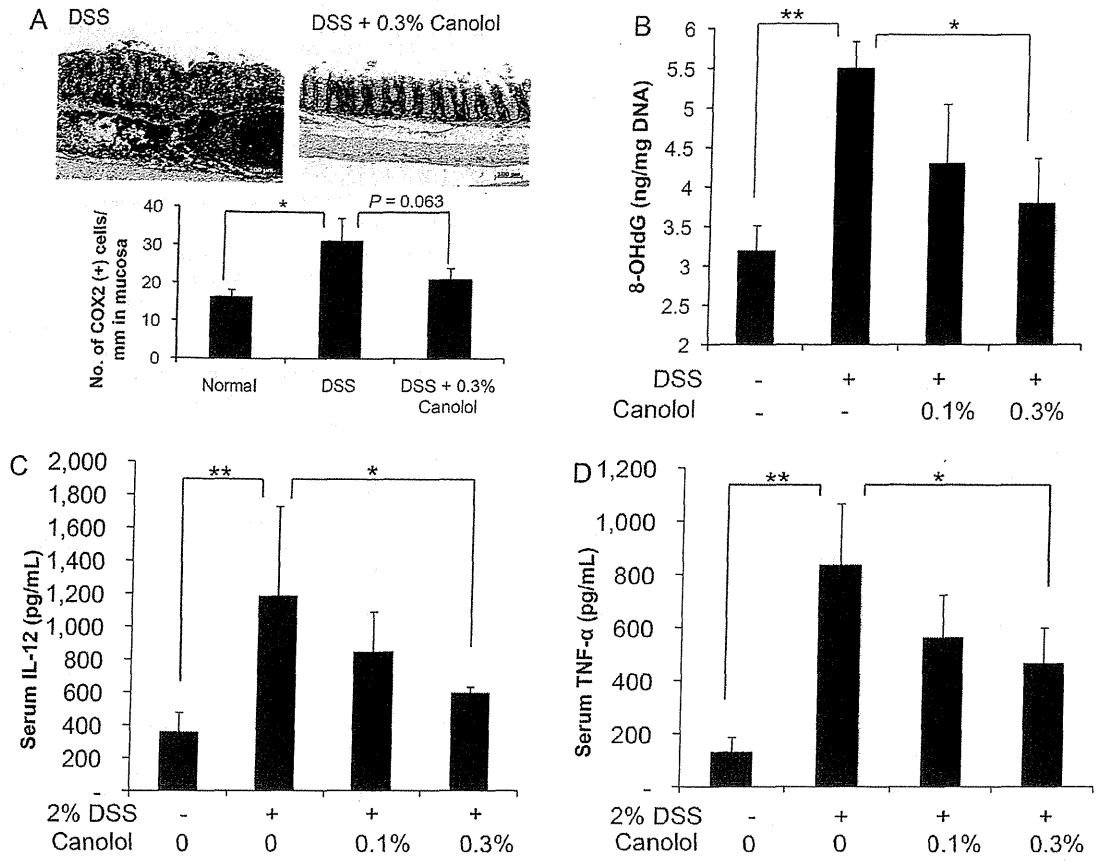

Fig. 2. Immunohistochemistry of COX-2 (**A**) in colorectal lesions, and plasma levels of 8-OHdG (**B**), as well as production of IL-12 (**C**) and TNF-α (**D**) in DSS-induced colitis and the protective effect of canolol. The protocols of DSS-induced colitis and canolol treatment are presented in Figure 1. Seven days after the start of DSS administration, mice were killed and serum samples were collected for measuring IL-12 and TNF-α by means of ELISA. See text for details. Data are means ± SD (n = 6–10). *P < 0.05, **P < 0.01.

TNF-α and iNOS in AOM/DSS-induced colon carcinogenesis. Similar to the findings in DSS colitis experiments (Figure 2A and D), significant decreases of TNF-α and iNOS expression were observed (Figure 4B and C). As to COX-2, though no significance was observed (P = 0.054), apparent lowered expression was found after feeding 0.3% of canolol (Figure 4A), and further immunohistochemical staining of COX-2 in colon mucosa also showed that average number of COX-2-positive cells in unit length tended to be lower at 0.46±0.31/mm in canolol group compared with 0.89±0.39/mm in AOM/DSS control group, although without statistical significance (data are mean ± SD; P = 0.082, Mann–Whitney U-test) (Figure 4E).

Moreover, when we examined the expression of HO-1, a major antioxidative antiapoptotic molecule in various tumors reflecting oxidative and other cellular stresses (25), a significantly decreased expression was observed in canolol group compared with AOM/DSS control group (Figure 4D), which in part supported the antioxidative effect of canolol, i.e. higher oxidative levels in AOM/DSS group inducing higher expression of HO-1, whereas suppressed oxidative stress by canolol resulted in lower expression of HO-1.

Effect of canolol on colon 26 solid tumor model

To further examine the effect of canolol on tumor growth, a syngeneic mouse colon tumor model (colon 26) was used. After oral administration of canolol (100 mg/kg) for three times, COX-2 expressions in tumors were significantly lowered (Figure 4F): average area of COX-2 was 1.42±0.47% in the control (no canolol) group, whereas 0.215±0.072% in the group fed with 0.3% canolol (data are mean ± SD; P < 0.002, Mann–Whitney U-test). However, only a slight but no significant suppression of tumor growth was found (Supplementary Figure 3, available at *Carcinogenesis* Online).

Safety of canolol

As summarized in Table II, no significant adverse effects such as decreases in red blood cell and white blood cell counts and hemoglobin levels were found in ICR mice after feeding 0.3% canolol for 6 weeks, which is the same dose for preventing AOM/DSS-induced colon carcinogenesis. Also, no significant changes in the liver enzymes and kidney functions were found under the same conditions.

Discussion

In this study, we demonstrated the protective effect of canolol, a potent antioxidant that was recently isolated from canola (rapeseed) oil (12), on IBD in a DSS-induced mouse model. Oral administration of a diet containing canolol to the mice significantly reduced the symptoms and suppressed the progression of this disease, as supported by the lengthening of the large bowel (Table I), as well as by reduced severity and numbers of ulcers in the colonic mucosa (Figure 1) and lower levels of COX-2 expression and inflammatory cytokines (Figure 2A, C and D). These findings were associated with a decreased occurrence of colon carcinogenesis induced by AOM/DSS (Table I). However, though suppression of COX-2 expression by canolol was also found in colon 26 solid tumor (Figure 4F), no significant delay of tumor growth was observed (Supplementary Figure 3,

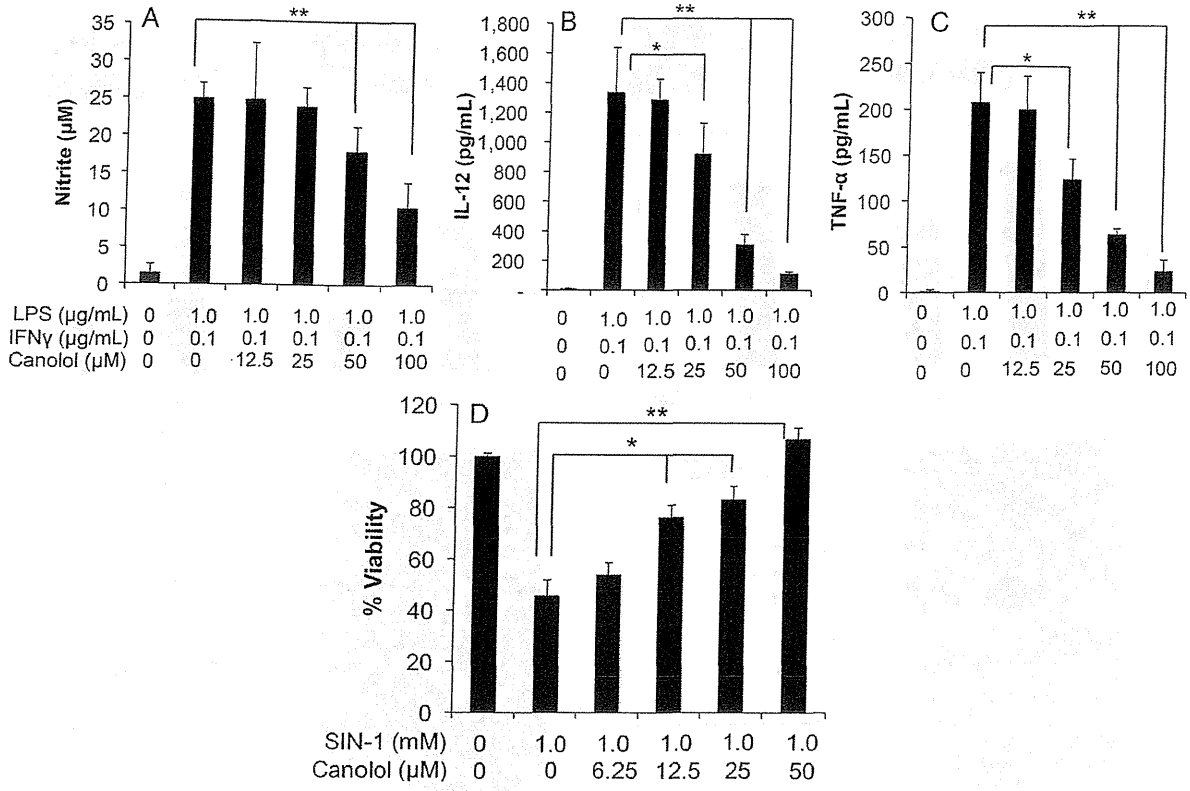

Fig. 3. Suppression of macrophage activation (**A**) and subsequent generation of IL-12 (**B**) and TNF-α (**C**), and cytoprotective effect against the toxicity of peroxynitrite ($ONOO^-$) in HEK293 (**D**) by canolol. Mouse macrophages were obtained from BALB/c mice. Macrophage activation, as generation of NO, was evaluated by using a Griess Reagent kit. IL-12 and TNF-α were measured using ELISA. See text for details. For cytotoxicity study, 3000 cells/well were plated in a 96-well plate. After overnight preincubation, 1 mM SIN-1 ($ONOO^-$ donor) was added to the cells. Different concentrations of canolol were administered. After an additional 48 h of incubation, cell viability was determined by using the 3-(4,5-dimethyl-2-thiazolyl)-2,5-diphenyl-2H-tetrazolium bromide (MTT) assay. Data are means ± SD ($n = 6–8$). $^*P < 0.05$, $^{**}P < 0.01$.

available at *Carcinogenesis* Online). Partly consistent with these findings, canolol does not show apparent cytotoxicity against cultured cells including colon cancer cells Caco-2 (Supplementary Figure 2, available at *Carcinogenesis* Online). These data suggested that canolol might not exhibit chemotherapeutic/cytotoxic effect against the growing tumors, whereas it exhibited significant chemopreventive effect probably during the stages of initiation and/or promotion via its antioxidative and anti-inflammatory activities.

Part of this anti-inflammatory effect of canolol may be attributable to its antioxidative or scavenging activity against the excess ROS that are produced during inflammation. ROS are known to be involved in many diseases including inflammation, infections, ischemia/reperfusion injury, neurological disorders, Parkinson's disease, hypertension and cancer (26–28). During the process of inflammation, O_2^- is extensively produced in infiltrated neutrophils and activated macrophages by means of reduced nicotinamide adenine dinucleotide phosphate oxidase and probably even more by xanthine oxidase, which is highly expressed in inflamed tissues (27–30). We described similar results in our previous study with an influenza virus infection model (29,31) and in our more recent study with a xanthine oxidase inhibitor in a rat liver ischemia/reperfusion model (30). Excess generation of ROS was also observed in DSS-induced colitis model and could be suppressed by xanthine oxidase inhibitor (Fang.J., Yin.H.Z., Liao.L., Qin.H.B., Ueda.F., Uemura.K., Eguchi.K., Bharate.G.Y., Nakamura.H., and Maeda.H., unpublished data). O_2^- is then converted to hydrogen peroxide by superoxide dismutase and/or glutathione peroxide, after which the hydrogen peroxide is converted to hydroxyl radicals in the presence of transition metals (e.g. Fe^{2+}). A massive amount of NO is also generated by iNOS that is upregulated in activated macrophages (22,28), and NO can react rapidly with O_2^- to form the more toxic species $ONOO^-$. All of these highly reactive biological radicals readily cross cell membranes and react with proteins, DNA and lipids (23,24,32–34), which results in cell damage. Furthermore, removal of NO by reaction with O_2^- on the vascular endothelial surface causes vasoconstriction and triggers neutrophil adherence and accumulation, which will promote the pathological process of inflammation (20,21). This notion is supported by results of the present study, in which canolol treatment significantly protected cells against the toxicity of $ONOO^-$ (Figure 4D and E), and moreover it also significantly decreased the levels of 8-OHdG, one of the major indicators of oxidative stress, in DSS-induced colitis model (Figure 2B).

Moreover, it was also reported that the antioxidative and cytoprotective effect of canolol is probably partly through upregulating antioxidative molecules such as NF-E2-related factor, HO-1, catalase and glutathione S-transferase-pi via an extracellular signal-regulated kinase-mediated pathway (35). However, in this study we found the decrease of HO-1 expression in the distal quarter of the colon where tumors occurred most frequently (Figure 4D). This finding may indicate the different expression profile of HO-1 in normal tissues and tumor tissues. In normal tissues, upregulated HO-1 protects against oxidative stress and other damages, whereas many tumors highly express HO-1 to support their rapid growth and protect against various oxidative stresses (25). Moreover, these findings partly agreed with a recent report showing that HO-1 may protect healthy tissues against carcinogen-induced injury, but in already growing tumors, it seems to favor their progression toward more malignant forms (36).

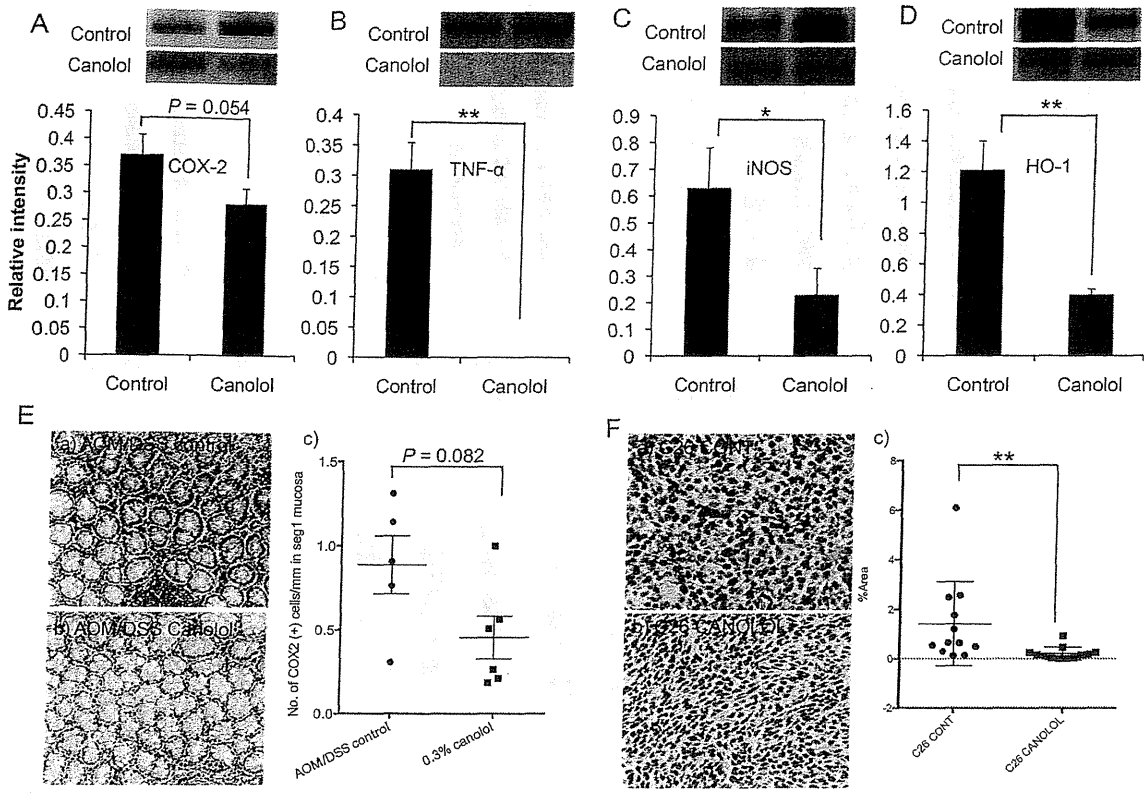

Fig. 4. Suppression of COX-2 (**A**), TNF-α (**B**) and iNOS (**C**) and upregulation of HO-1 by canolol as evaluated by reverse transcription–polymerase chain reaction, and the decreased COX-2 expression in colon tissue of AOM/DSS-treated ICR mice (**E**) and colon 26 (C26) mouse tumor (**F**) *in vivo* after canolol treatment. In (**A–D**), two representative DNA bands of each group (control and canolol group) are shown, and the results were semiquantitated as relative intensity compared with the intrinsic DNA expression of GAPDH as control. Immunohistochemical staining of COX-2 in colon tissue of AOM/DSS control mice (E-a) and canolol-treated mice (E-b) is shown in (E), and that in C26 tumor tissues without and with canolol treatment is shown in (F-a) and (F-b), respectively; in both cases, the COX-2-positive (brown colored) area was quantitated (E-c and F-c). See text for details. Data are means ± SD ($n = 5–12$). $^{*}P < 0.05$, $^{**}P < 0.01$ by Mann–Whitney *U*-test.

Table II. Change in RBC, WBC, hemoglobin and plasma liver enzyme levels and kidney function after feeding canolol (0.3% for 6 weeks) in ICR mice[a]

	RBC (10^4/μl)		WBC (10^2/μl)		Hb (g/dl)
Normal	992.2±35.9		30.4±4.2		16.0±0.6
Canolol[b]	953.0±20.2		28.8±1.9		15.1±0.4
	BUN (mg/dl)	Cr (mg/dl)	AST (IU/l)	ALT (IU/l)	LDH (IU/l)
Normal	20.7±0.8	0.15±0.02	67.3±2.8	28.4±2.2	1383.0±54.7
Canolol[b]	21.5±1.3	0.13±0.01	65.1±4.5	37.6±4.2	1036.4±149.3

ALT, alanine aminotransferase; AST, aspartate aminotransferase; BUN, blood urea nitrogen; Cr, creatinine; Hb, hemoglobin; LDH, lactate dehydrogenase; RBC, red blood cells; WBC, white blood cells.
[a]No significant difference was found between canolol feeding mice and normal mice in all selected indices. Values are presented as means ± SE, $n = 5–8$.
[b]Canolol was administered at 0.3% (w/w) in diet. Assays were carried out at 6 weeks after feeding canolol.

Taken together, the association of canolol with HO-1 in AOM/DSS colon carcinogenesis seems to be different from that in normal tissues during stresses and damages as described earlier (35); further investigations are thus warranted to make clear the mechanisms involved in the effect of canolol in different conditions.

COX-2 is the enzyme that catalyzes the conversion of arachidonic acid to prostaglandins, it is unexpressed under normal conditions in most cells, but elevated levels are found under inflammatory condition and is thus largely responsible for causing inflammation (37). Many studies revealed that the products of COX-2 prostaglandins are highly involved in the carcinogenesis of many tumors including colorectal cancer metastasis and tongue and esophageal cancers (38,39). In this study, we found a decrease in COX-2 expression (both in mRNA and protein levels) after canolol treatment, though not statistically significant, in DSS-induced colitis (Figure 2A) and in AOM/DSS-induced colon carcinogenesis (Figure 4A). These findings at least partly suggested that suppression of COX-2 expression is probably involved in the effect of canolol on DSS-induced colitis and colon carcinogenesis.

Both the present study and our previous study (16) of canolol *in vivo* showed suppression of a number of inflammatory mediators

such as TNF-α, IL-12, IL-1β, iNOS and COX-2 (Figure 2A, C, and D, Figure 4A–C and ref. 16), which confirms that this suppression will contribute to the anti-inflammatory activity and the antioxidative effect of canolol against IBD and the subsequent colon carcinogenesis. Infiltrated neutrophils and activated macrophages are major producers of these inflammatory cytokines during inflammatory diseases including IBD (40,41). ROS play an important initial role in both the activation of macrophages and the induction of inflammatory cytokines. Bulua et al. (42) recently reported that ROS are crucial in LPS-stimulated macrophages for inducing production of several proinflammatory cytokines through an mitogen-activated protein kinase signaling pathway, as an essential feature of innate immunity. Apoptosis signal-regulating kinase 1 is also involved in this immune response (43). Consistent with this result, we found in this study that the ROS scavenger canolol suppressed activation of macrophages stimulated by LPS and interferon-γ, as evidenced by reduced NO generation (Figure 3A) and lower levels of IL-12 and TNF-α (Figure 3B and C). Also, certain cytokines, i.e. TNF-α and IL-12, secreted by activated phagocytic cells, can enhance ROS generation (44,45), which explains the important role of cytokines in the pathogenic process of inflammation. These findings suggested that the chemopreventive effect of canolol is mostly via its antioxidative and anti-inflammatory effect to inhibit the oxidative stress and inflammation, thus inhibiting the carcinogenesis cascades.

Canolol is extracted from crude canola oil after roasting the rape seeds and is a naturally occurring compound in this edible oil whose concentration is estimated to be ~220–1200 ppm (12), which could provide doses similar to that used in our study. The amounts of canolol administered orally in the diet in this study were 0.1% and 0.3%, or equivalent to 1–3 g/kg (dry weight) of feed for humans, which is a reasonable range for supplement diet. In our previous study, we also applied the 0.1% concentration in an *H.pylori*-induced gastric carcinogenesis model and showed a significant cancer-preventive effect (15). Because the present colon carcinogenesis prevention study revealed no dose dependency (Table I), the 0.1% canolol concentration may be the level of saturation. That is, 0.1% canolol may be sufficient to prevent colon carcinogenesis.

Furthermore, canolol showed very little cytotoxicity to cells in culture: it had no apparent toxicity in human HEK293 cells at least up to 100 μM, in human Caco-2 cells up to 200 μM (Supplementary Figure 2B and C, available at *Carcinogenesis* Online) or in macrophages up to 300 μM (0.054 mg/ml), as described previously (16) and in present study (Supplementary Figure 2A, available at *Carcinogenesis* Online), which is a far higher concentration than the concentration for effective scavenging of ROS (i.e. 1–20 μM) (12,46). Similar results were obtained in our *in vivo* study. Mice receiving a diet containing canolol up to 0.3% for 6 weeks showed no apparent change in body weight (Table II) and no apparent toxicity as reflected by blood cell count and biochemistry of liver and kidney functions (Table II). This safety profile suggests that canolol has the potential to be not only a drug but also a food supplement for disease prevention.

Colon cancer is the most common type of cancer in developed countries, with the highest incidence and mortality rates (47). With regard to the mechanisms of colon carcinogenesis, genetic factors seem to play an important role, as in familial adenomatous polyposis (48). However, ROS were recently found to be one of the critical factors in colon carcinogenesis and in familial adenomatous polyposis (49). Dietary habits are known to be highly associated with the occurrence of colon cancer (50,51). For example, oxidized oils in high-fat diets, which are a risk factor for colon cancer, generate lipid peroxyl radicals in the presence of heme or iron, damage DNA and consequently induce colon cancer (50). Also, ROS contribute to many conditions other than inflammation, such as virus infections and ischemia/reperfusion injury, as described above.

Moreover, an unhealthy diet, with a low consumption of green vegetables and thus less antioxidants, may lead to the adverse consequences of these ROS-related diseases. It should be noted that purified canola oil that is available in large supermarkets does not contain canolol because the refining process removes it (12). It should be also noted that the content of canolol increases dramatically by roasting process as used in traditional oil refining process (12). Thus, the refining process should be modified so that canolol is retained. The canolol used in this study was synthesized, so synthetic canolol may be used as a preventive agent for these diseases.

For IBD treatment, drugs commonly used in clinical settings provide symptomatic or palliative relief. Canolol treatment, however, aims more at the cause of the disease, i.e. ROS. All these data therefore suggest that canolol may be effective not only for IBD-associated colon cancer but also for ROS-dependent carcinogenesis, as described for gastric cancer involving *H.pylori* infection (16). Canolol thus holds promise as a preventive agent or supplement for both IBD and colon cancer.

Supplementary material

Supplementary Figures 1–3 can be found at http://carcin.oxfordjournals.org/

Funding

Grants-in-Aid from the Ministry of Education, Science, Culture, Sports and Technology of Japan (No. 08011717); Cancer Speciality grant from the Ministry of Health, Welfare and Labour (H23-3rd Cancer Project-General-001); research funds of the Faculty of Pharmaceutical Sciences at Sojo University (RW15000025).

Acknowledgements

The authors thank Ms Masayo Idenoue for her excellent technical assistance.

Conflict of Interest Statement: None declared.

References

1. Baumgart,D.C. *et al.* (2007) Inflammatory bowel disease: cause and immunobiology. *Lancet*, **369**, 1627–1640.
2. Baumgart,D.C. *et al.* (2007) Inflammatory bowel disease: clinical aspects and established and evolving therapies. *Lancet*, **369**, 1641–1657.
3. Xavier,R.J. *et al.* (2007) Unravelling the pathogenesis of inflammatory bowel disease. *Nature*, **448**, 427–434.
4. Khor,B. *et al.* (2011) Genetics and pathogenesis of inflammatory bowel disease. *Nature*, **474**, 307–317.
5. Ohkusa,T. *et al.* (2004) The role of bacterial infection in the pathogenesis of inflammatory bowel disease. *Intern. Med.*, **43**, 534–539.
6. Arthur,J.C. *et al.* (2012) Intestinal inflammation targets cancer-inducing activity of the microbiota. *Science*, **338**, 120–123.
7. Ohkusa,T. *et al.* (2005) Effectiveness of antibiotic combination therapy in patients with active ulcerative colitis: a randomized, controlled pilot trial with long-term follow-up. *Scand. J. Gastroenterol.*, **40**, 1334–1342.
8. Ohkusa,T. *et al.* (2010) Newly developed antibiotic combination therapy for ulcerative colitis: a double-blind placebo-controlled multicenter trial. *Am. J. Gastroenterol.*, **105**, 1820–1829.
9. Rezaie,A. *et al.* (2007) Oxidative stress and pathogenesis of inflammatory bowel disease: an epiphenomenon or the cause? *Dig. Dis. Sci.*, **52**, 2015–2021.
10. Pavlick,K.P. *et al.* (2002) Role of reactive metabolites of oxygen and nitrogen in inflammatory bowel disease. *Free Radic. Biol. Med.*, **33**, 311–322.
11. Yukitake,H. *et al.* (2011) BTZO-15, an ARE-activator, ameliorates DSS- and TNBS-induced colitis in rats. *PLoS One*, **6**, e23256.
12. Wakamatsu,D. *et al.* (2005) Isolation, identification, and structure of a potent alkyl-peroxyl radical scavenger in crude canola oil, canolol. *Biosci. Biotechnol. Biochem.*, **69**, 1568–1574.
13. Shrestha,K. *et al.* (2012) Isolation and identification of a potent radical scavenger (canolol) from roasted high erucic mustard seed oil from Nepal and its formation during roasting. *J. Agric. Food Chem.*, **60**, 7506–7512.

14. Kuwahara,H. *et al.* (2004) Antioxidative and antimutagenic activities of 4-vinyl-2,6-dimethoxyphenol (canolol) isolated from canola oil. *J. Agric. Food Chem.*, **52**, 4380–4387.
15. Kuwahara,H. *et al.* (2009) Generation of drug-resistant mutants of *Helicobacter pylori* in the presence of peroxynitrite, a derivative of nitric oxide, at pathophysiological concentration. *Microbiol. Immunol.*, **53**, 1–7.
16. Cao,X. *et al.* (2008) 4-Vinyl-2,6-dimethoxyphenol (canolol) suppresses oxidative stress and gastric carcinogenesis in *Helicobacter pylori*-infected carcinogen-treated Mongolian gerbils. *Int. J. Cancer*, **122**, 1445–1454.
17. Wirtz,S. *et al.* (2007) Chemically induced mouse models of intestinal inflammation. *Nat. Protoc.*, **2**, 541–546.
18. Neufert,C. *et al.* (2007) An inducible mouse model of colon carcinogenesis for the analysis of sporadic and inflammation-driven tumor progression. *Nat. Protoc.*, **2**, 1998–2004.
19. Takagi,T. *et al.* (2011) Carbon monoxide liberated from carbon monoxide-releasing molecule exerts an anti-inflammatory effect on dextran sulfate sodium-induced colitis in mice. *Dig. Dis. Sci.*, **56**, 1663–1671.
20. Akaike,T. *et al.* (2000) Nitric oxide and virus infection. *Immunology*, **101**, 300–308.
21. Beckman,J.S. *et al.* (1996) Nitric oxide, superoxide, and peroxynitrite: the good, the bad, and ugly. *Am. J. Physiol.*, **271**(5 Pt 1), C1424–C1437.
22. Akaike,T. *et al.* (1996) Pathogenesis of influenza virus-induced pneumonia: involvement of both nitric oxide and oxygen radicals. *Proc. Natl Acad. Sci. USA*, **93**, 2448–2453.
23. Niles,J.C. *et al.* (2006) Peroxynitrite-induced oxidation and nitration products of guanine and 8-oxoguanine: structures and mechanisms of product formation. *Nitric Oxide*, **14**, 109–121.
24. Sawa,T. *et al.* (2006) Nitrative DNA damage in inflammation and its possible role in carcinogenesis. *Nitric Oxide*, **14**, 91–100.
25. Fang,J. *et al.* (2004) Antiapoptotic role of heme oxygenase (HO) and the potential of HO as a target in anticancer treatment. *Apoptosis*, **9**, 27–35.
26. McCord,J.M. (2000) The evolution of free radicals and oxidative stress. *Am. J. Med.*, **108**, 652–659.
27. Maeda,H. *et al.* (1991) Oxygen free radicals as pathogenic molecules in viral diseases. *Proc. Soc. Exp. Biol. Med.*, **198**, 721–727.
28. Maeda,H. *et al.* (1998) Nitric oxide and oxygen radicals in infection, inflammation, and cancer. *Biochemistry (Mosc).*, **63**, 854–865.
29. Akaike,T. *et al.* (1990) Dependence on O2- generation by xanthine oxidase of pathogenesis of influenza virus infection in mice. *J. Clin. Invest.*, **85**, 739–745.
30. Fang,J. *et al.* (2010) Tissue protective effect of xanthine oxidase inhibitor, polymer conjugate of (styrene-maleic acid copolymer) and (4-amino-6-hydroxypyrazolo[3,4-*d*]pyrimidine), on hepatic ischemia-reperfusion injury. *Exp. Biol. Med. (Maywood)*, **235**, 487–496.
31. Oda,T. *et al.* (1989) Oxygen radicals in influenza-induced pathogenesis and treatment with pyran polymer-conjugated SOD. *Science*, **244**, 974–976.
32. Davies,K.J. (1993) Protein modification by oxidants and the role of proteolytic enzymes. *Biochem. Soc. Trans.*, **21**, 346–353.
33. Lindahl,T. (1993) Instability and decay of the primary structure of DNA. *Nature*, **362**, 709–715.
34. Wagner,B.A. *et al.* (1994) Free radical-mediated lipid peroxidation in cells: oxidizability is a function of cell lipid bis-allylic hydrogen content. *Biochemistry*, **33**, 4449–4453.
35. Dong,X. *et al.* (2011) Protective effect of canolol from oxidative stress-induced cell damage in ARPE-19 cells via an ERK mediated antioxidative pathway. *Mol. Vis.*, **17**, 2040–2048.
36. Was,H. *et al.* (2011) Effects of heme oxygenase-1 on induction and development of chemically induced squamous cell carcinoma in mice. *Free Radic. Biol. Med.*, **51**, 1717–1726.
37. Dubois,R.N. *et al.* (1998) Cyclooxygenase in biology and disease. *FASEB J.*, **12**, 1063–1073.
38. Hawcroft,G. *et al.* (2012) The omega-3 polyunsaturated fatty acid eicosapentaenoic acid inhibits mouse MC-26 colorectal cancer cell liver metastasis via inhibition of PGE2-dependent cell motility. *Br. J. Pharmacol.*, **166**, 1724–1737.
39. Miyamoto,S. *et al.* (2008) A novel rasH2 mouse carcinogenesis model that is highly susceptible to 4-NQO-induced tongue and esophageal carcinogenesis is useful for preclinical chemoprevention studies. *Carcinogenesis*, **29**, 418–426.
40. Nathan,C. (2006) Neutrophils and immunity: challenges and opportunities. *Nat. Rev. Immunol.*, **6**, 173–182.
41. Mosser,D.M. *et al.* (2008) Exploring the full spectrum of macrophage activation. *Nat. Rev. Immunol.*, **8**, 958–969.
42. Bulua,A.C. *et al.* (2011) Mitochondrial reactive oxygen species promote production of proinflammatory cytokines and are elevated in TNFR1-associated periodic syndrome (TRAPS). *J. Exp. Med.*, **208**, 519–533.
43. Matsuzawa,A. *et al.* (2005) ROS-dependent activation of the TRAF6-ASK1-p38 pathway is selectively required for TLR4-mediated innate immunity. *Nat. Immunol.*, **6**, 587–592.
44. Warren,J.S. *et al.* (1988) Macrophage-derived cytokines amplify immune complex-triggered O2-. responses by rat alveolar macrophages. *Am. J. Pathol.*, **130**, 489–495.
45. Szefler,S.J. *et al.* (1989) IFN-gamma and LPS overcome glucocorticoid inhibition of priming for superoxide release in human monocytes. Evidence that secretion of IL-1 and tumor necrosis factor-alpha is not essential for monocyte priming. *J. Immunol.*, **142**, 3985–3992.
46. Galano,A. *et al.* (2011) Canolol: a promising chemical agent against oxidative stress. *J. Phys. Chem. B*, **115**, 8590–8596.
47. Jemal,A. *et al.* (2010) Global patterns of cancer incidence and mortality rates and trends. *Cancer Epidemiol. Biomarkers Prev.*, **19**, 1893–1907.
48. Strate,L.L. *et al.* (2005) Hereditary colorectal cancer syndromes. *Cancer Causes Control*, **16**, 201–213.
49. Ullman,T.A. *et al.* (2011) Intestinal inflammation and cancer. *Gastroenterology*, **140**, 1807–1816.
50. Sawa,T. *et al.* (1998) Lipid peroxyl radicals from oxidized oils and heme-iron: implication of a high-fat diet in colon carcinogenesis. *Cancer Epidemiol. Biomarkers Prev.*, **7**, 1007–1012.
51. Chao,A. *et al.* (2005) Meat consumption and risk of colorectal cancer. *JAMA*, **293**, 172–182.

Received December 13, 2012; revised July 8, 2013; accepted July 23, 2013

RESEARCH ARTICLE

Inflammation Enhanced X-irradiation-Induced Colonic Tumorigenesis in the Min mouse

Ayumi Nojiri[1,2], Takeshi Toyoda[1,3], Takuji Tanaka[4], Toshimichi Yoshida[2], Masae Tatematsu[1], Tetsuya Tsukamoto[1,2,5]*

Abstract

Inflammation is potential risk factor of various human malignancies. Inflammatory bowel syndromes such as ulcerative colitis are well known as risk factors for colon cancer. Here, we examined enhancing effects of dextran sulfate sodium (DSS)-associated inflammation on X-irradiation induced colonic tumorigenesis in Min and wild-type (WT) mice. Animals were X-irradiated at 1.5 Gy at 5 weeks of age (at 0 experimental week) and 2% DSS in drinking water was administered at 5 or 11 experimental weeks. Mice were sacrificed at 16 weeks and incidence and multiplicity of colonic tumors were assessed. Incidence of colonic tumors in Min mouse was increased from 33.3% to 100% ($p<0.05$) with X-irradiation alone, whereas no tumors were developed in WT mice. In DSS-treated Min mice, X-irradiation increased the number of colonic tumors. Total number of colonic tumors was increased 1.57 times to 30.7±3.83 tumors/mouse with X-irradiation+DSS at 5 weeks comapared to 19.6±2.9 in corresponding DSS alone group ($p<0.05$). When the duration of inflammation was compared, longer period of DSS effect promoted more colonic tumorigenesis. Collectively, we conclude that X-irradiation and DSS-induced inflammation act synergistically for colonic tumorigenesis.

Keywords: Min mouse - X-irradiation - DSS - colon

Asian Pac J Cancer Prev, **14** (7), 4135-4139

Introduction

Inflammation has been widely known as strong risk and promoting factor of carcinogenesis (Balkwill and Mantovani, 2001) in various types of human cancers (Ohshima et al., 2003). Among them, ulcerative colitis is in high risk condition in colonic carcinogensis (Munkholm, 2003). In the animal counterpart, dextran sulfate sodium (DSS) (Okayasu et al., 1990) showed powerful tumor promoting effect in murine colonic carcinogenesis models initiated with azoxymethane (AOM) (Tanaka et al., 2003), 1,2-dimethylhydrazine (DMH) (Kohno et al., 2005), and 2-amino-1-methyl-6-phenylimidazo[4,5-b]pyridine (PhIP) (Tanaka et al., 2005).

Familial adenomatous polyposis (FAP) is an inherited human disease characterized by numerous colorectal tumorigenesis (Kinzler and Vogelstein, 1996). FAP is caused by mutation in the adenomatous polyposis coli (APC) tumor suppressor gene (Powell et al., 1993). Min (multiple intestinal neoplasia) mouse is a murine model of human FAP (Moser et al., 1990), which has nonsense mutation at codon 850 in Apc gene (Su et al., 1992). The mouse develops multiple intestinal adenomas with inactivation of wild type allele. Min mouse have been revealed to be highly susceptible to carcinogenic agents. Subcarcinogenic low-dose *N*-ethyl-*N*-nitrosourea (ENU) increased the tumor incidence in the intestine and mammary gland in Min mice (Shoemaker et al., 1995). Other colonic carcinogens including PhIP (Steffensen et al., 1997) and AOM (Paulsen et al., 2003) also increased intestinal tumors. Besides chemical carcinogens, Min mice have been revealed to be susceptible to ionizing radiation (Luongo and Dove, 1996) in the age-dependent manner (Okamoto and Yonekawa, 2005). Inflammatory stimuli by DSS strongly induced colonic neoplasia in Min mice (Tanaka et al., 2006).

In this study, we investigated whether DSS-induced inflammation enhanced colorectal tumorigenesis initiated with low-dose X-irradiation in Min mice.

Materials and Methods

Animals and genotyping

Male C57BL/6J-ApcMin/J (Min) mice were purchased from The Jackson Laboratory (Bar Harbor, Maine, USA). Female wild type (WT) C57BL6/J were obtained from Clea Japan (Tokyo, Japan). They were housed in plastic cages with hardwood chips in an air-conditioned room

[1]*Division of Oncological Pathology, Aichi Cancer Center Research Institute, Nagoya,* [2]*Department of Pathology and Matrix Biology, Mie University Graduate School of Medicine, Tsu,* [3]*Division of Pathology, National Institute of Health Sciences, Tokyo,* [4]*The Tohkai Cytopathology Institute, Cancer Research and Prevention, Gifu,* [5]*Department of Diagnostic Pathology, Fujita Health University School of Medicine, Toyoake, Japan* **For correspondence: ttsukamt@fujita-hu.ac.jp*

with 12 h light-12 h dark cycle and were given basal diet (OA-2, Clea Japan) and water *ad libitum*. One male Min mouse and 5 female wild type C57BL6/J were mated and offsprings were subjected to genotyping. DNA samples were extracted from their tails using a QIAamp tissue kit (QIAGEN, Tokyo, Japan). The 10 μl PCR reaction mixture consited of TITANIUM Taq DNA polymerase (Clontech, Mountain View, CA, USA), 1x buffer provided, 1x dNTP, 1μM of PCR primers (named oIMR0033, oIMR0034, and oIMR0758) and 1μl of genomic DNA. oIMR0033 (5'- GCC ATC CCT TCA CGT TAG -3') and oIMR0034 (5'- TTC CAC TTT GGC ATA AGG C -3') are forward and reverse wild type primers, respectively, to amplify common region. oIMR0758 is forward Min specific primer (5'- TTC TGA GAA AGA CAG AAG TTA -3') in which final adenosin residue corresponds to the mutation. PCR was performed using a Veriti thermal cycler (Applied Biosystems, Life Technologies, Carlsbad, CA, USA) as follows: 1 cycle of 95°C for 1 min; 35 cycles of 95°C for 30 sec, 65°C for 30 sec, 68°C for 30 sec; 1 cycle of 68°C for 3 min. The reaction mixture was electrophoresed in 0.8% SeaKem GTG agarose gel (Cambrex, East Rutherford, NJ, USA). Animals were judged as Min, if 340 bp band was appeared; both of wild type and Min genotypes possessed 600 bp band encompassing the mutation residue.

Experimental design

The experimental design is shown in Figure 1. Min mice and littermate WT mice were randomly divided into 6 groups (groups A–D). Single whole-body irradiation was given to five week-old animals at 1.5 Gy using an X-ray irradiator (MBR-1520R-3, Hitachi Power Solutions Co., Ltd., Tokyo, Japan) with a 0.5 mm Al+0.2 mm Cu filter in Groups C, D, and F. Dose of X-irradiation was determined to be lower than the previous report (Okamoto and Yonekawa, 2005) to compare enhancing effect of dextran sulfate sodium (DSS). DSS with a molecular weight of 40,000 was purchased from ICN Biochemicals, Inc. (Aurora, OH, USA), dissolved in water at a concentration of 2% (w/v), and administered at 5 experimental week in Groups E and F or at 11 week in Groups B and D for 1 week. The animals were sacrificed at 16 week. Total colon and cecum were fixed in 10% neutral buffered formalin or methacarn and stained with 0.2% methylene blue. Colon segments (S) were divided from S1 to S4 and cecum as S5 (Figure 2). The number of colonic tumors was counted in each segment. The experimental design was approved by the Animal Care Committee of the Aichi Cancer Center Research Institute, and the animals were cared for in accordance with institutional guidelines as well as the Guidelines for Proper Conduct of Animal Experiments (Science Council of Japan, June 1, 2006).

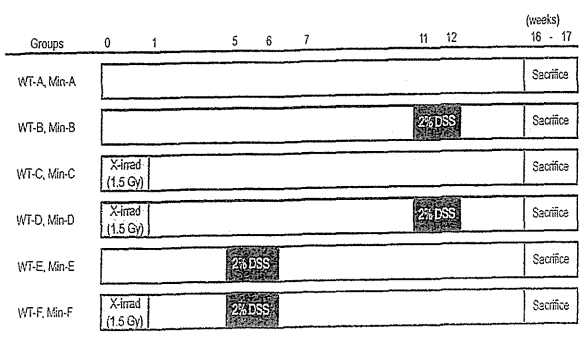

Figure 1. Experimental Protocol

Statistical analysis

The significance of difference in the incidence of colonic tumors was calculated using Fischer's exact test. Tumor multiplicities were analyzed with Mann-Whitney *U* test. Differences were considered as statistically significant if $p<0.05$.

Results

Incidence of colon tumors in WT and Min mice

Effective numbers of animals are described in Table 1. In the wild type mice, incidence of Group WT-D (33.3%) is significantly higher than that of Group WT-C (0%), suggesting enhancing results of DSS on X-irradiated tumorigenesis ($p<0.05$).

When Groups Min-A and Min-C were compared in Min mice, incidence of Group C (100%) was higher than that of Group A (33.3%), proving the aggravating effect of X-irradiation especially in Min mice ($p<0.002$).

When the two genotypes were compared in each group, Min mice showed increased incidence with statistical significance in Groups B-F (Table 1).

Multiplicity of colon tumors in Min mice

X-irradiation at 1.5 Gy alone [the number of tumors=0.91±0.21 (Ave±SE)/mouse in Group C] increased the number of colon tumors in S2 compared with the corresponding region in Group A (0.25±0.13/mouse, $p<0.05$). Total number was also augmented (2.55±0.41 and 1.33±0.45/mouse in Groups C and A, respectively,

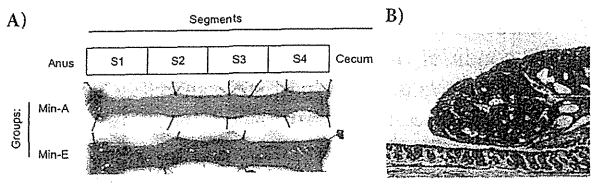

Figure 2. Macroscopic View and Histology of Colon Tumor. A) Macroscopic view of colonic mucosa. Total colon is divided to S1-S4. Cecum is S5 (not shown). Methylene blue staining. **B)** Representative histology of colonic tumor. Hematoxylin and eosin staining. Original magnification, 50x

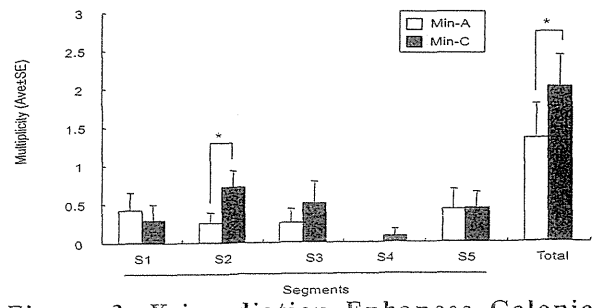

Figure 3. X-irradiation Enhances Colonic Tumorigenesis in Min mice without DSS. Group Min-A (Open bar) and Min-C (Closed bar). *$p<0.05$

Table 1. Incidence of Colon Tumors

		WT		Min		WT vs. Min
		Effective No. (male/female)	No. of mice with colon tumors (Incidence)	Effective No. (male/female)	No. of mice with colon tumors (Incidence)	
Groups	A	12 (6/6)	0 (0%)	12 (10/2)	4 (33.3%)	p=0.09
	B	14 (7/7)	3 (21.4%)	9 (4/5)	9 (100%)	p<0.002
	C	17 (8/9)	0 (0%)	11 (4/7)	11 (100%)**	p<0.0001
	D	9 (3/6)	3 (33.3%)*	8 (3/5)	8 (100%)	p<0.001
	E	15 (9/6)	0 (0%)	7 (3/4)	7 (100%)	p<0.0001
	F	10 (5/5)	2 (20.0%)	6 (5/1)	6 (100%)	p<0.001

*p<0.05 vs. WT-C, **p<0.002 vs. Min-A

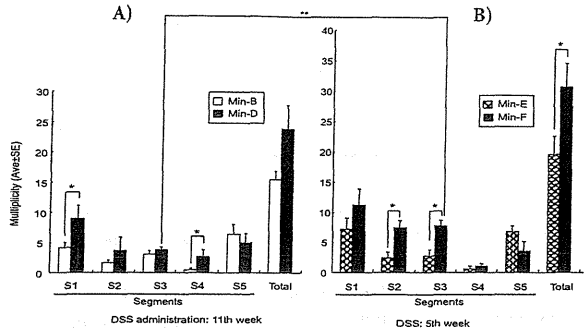

Figure 4. X-irradiation Promoted Colonic Tumorigenesis in DSS Treated Min mice. Group Min-B (Open bar), Min-D (Hatched bar), Min-E (Cross-hatched bar), and Min-F (Closed bar). *p<0.05 and **p<0.01

p<0.05) (Figure 3).

When 2% DSS was administered at 11 experimental week (Groups B and D), the number of colonic tumors were 8.88±2.20 (p<0.05) and 2.63±1.15 (p<0.05) in S1 and S4 in Group D, compared to 4.11±0.87 and 0.44±0.24, respectively, in Group B. It suggested enhancing effect of X-irradiation in Group D (Figure 4A).

If DSS was given at 5 week (Groups E and F), the numbers were 7.33±1.26 and 7.67±0.96 in S2 and S3, respectively, in Group F, compared with 2.43±0.87 and 2.71±1.04 in Group E, also indicating stimulating effect of X-irradiation in Group F (Figure 4B). Total numbers of colonic tumors was 30.67±3.83 and 19.57±2.9 in Groups F and E, respecively; the former was significantly higher than the latter (p<0.01).

When the two X-irradiation+DSS groups (Groups D and F in Figure 4 crossing left and right panels) were compared, earlier administration of DSS (7.67±0.96, Group F) was more effective in increment of colonic tumors in S3 compared to Group D (3.75±0.45) (p<0.05).

Multiplicity of colon tumors in WT mice

The number of total colonic tumors were 0.00±0.00, 0.50±0.27, 0.00±0.00, 0.78±0.46, 0.00±0.00, and 0.20±0.13/mouse in Groups A, B, C, D, E, and F, respecively, showing no significant differences among these groups.

Discussion

In the present study, we analyzed promoting effect of DSS-induced inflammation on X-irradiated colorectal carcinogenesis in WT and Min mice. Firstly, X-irradiation alone without DSS was assessed to confirm the effect of X-irradiation. In the Min mouse, incidence of colonic tumors was increased to 100% compared to non-irradiated group (33.3%). The number of colonic tumors in S2 was also increased with X-irradiation compared with non-irradiated Min mice. On the other hand, WT mice were not influenced with X-irradiation. It suggested that *Apc* locus might be more sensitive to loose normal APC function in Min mice although chromosome abberation might have occurred independent of their sequence (Rydberg, 1996). Okamoto and Yonekawa (Okamoto and Yonekawa, 2005) reported that 10 days old Min mice were more sensitive than other ages. In this study, since the mice were X-irradiated around 5 weeks old (35 days old), enhancing effect may have become unclear.

In the Min mice, DSS alone has known to enhance colonic tumorigenesis (Tanaka et al., 2006). X-irradiation was further added to assess if it may have enhanced colonic tumorigenesis. When Group F was compared with E, tumor multiplicity was increased in S2 and S3. Then, Group D vs. B, the number of tumors was increased upon X-irradiation in S1 and S4. Although localization of colonic tumors were different, X-irradiation was proved to exacerbate DSS-associated colonic tumorigenesis in Min mice. When the timing of DSS treatment was compared whether duration of inflammation could affect promoting effect, longer duration of inflammation had more enhancing effect (Group F) compared with shorter period (Group D). Similar phenomenon was observed in carcinogen induced murine colonic carcinogenesis model (Tanaka et al., 2003) and DSS alone induced model (Tanaka et al., 2006).

Considering WT mice, tumor incidence was increased in Groups D and F compared with non-treated or X-irradiation alone Groups, although enhancing effect was not as clear as that of Min mice. It was suggested that DSS treatment could bring latent genetic damage to apparent colonic tumors.

In the serial research in Life Span Study cohort of atomic bomb surviviors (Ozasa et al., 2012), the additive radiation risk of solid cancers continues to increase throughout life with a linear dose-response relationship. The estimated lowest dose range with a significant excessive relative risk (ERR) for all solid cancer was 0 to 0.20 Gy indicating no threshold. The risk of cancer mortality increased significantly for most major sites, including colon, whereas rectum did not. In the current study, multiplicities of colonic tumors (S2-S4 regions) were significantly increased with X-irradiation in Min-C (S2), Min-D (S4), and Min-F (S2 and S3) groups. In the

rectum (S1 region), although tumor multiplicity was not significantly different in DSS non-treated groups between Min-C and Min-A regardless of X-irradiation, Min-D receiving X-irradiation showed higher tumor multiplicity in the rectum compared with Min-B group. It suggested DSS-induced inflammation might have influenced rectal tumorigenesis as well as in colon.

Exposure to ionizing radiation is associated with an increased risk of cancer. The majority of radiation exposure and risk associated with gastrointestinal malignancy comes from CT scans, especially of the abdomen and pelvis; the colon carries the highest lifetime attributable risk of radiation associated malignancy (Chang and Hou, 2011). Besides patients, cancer risk of colon and rectum cancers in male diagnostic radiation workers in Korea also showed a significantly increasing trend according to the increase of the average annual radiation dose (HR: 2.37) (Choi et al., 2013).

Oncology patients treated for childhood cancer tended to develop secondary colorectal carcinomas. This risk was reported to be proportional to dose and volume of radiation; tumors were more likely localized in an irradiated segment of the colon (Nottage et al., 2012). Radiotherapy is a powerful tool for the treatment of gynecological malignancies including cervical (Tamai et al., 1999) and endemetrial cancers (Brown et al., 2010) and prostate cancer (Bolla et al., 2013). Patients treated with radiotherapy likely have significantly increased risk of subsequent primary malignancies including bladder, vagina, colon, and soft-tissue (Brown et al., 2010).

Low-level ionizing radiation (mean colon dose=0.18 Gy) has been revealed to influence the development of soft tissue sarcomas in atomic bomb survivors (Samartzis et al., 2013). However, no sarcomas were found in the current study, suggesting the DSS-induced inflammation has rarely affect stromal cells at least in this experimental condition.

In summary, our results suggest that colonic inflammation enhanced occult X-irradiated tumorigenesis not only in Min mice but also WT animals. It should be noted that those with colorectal inflammation including inflammatory bowel disease might exacerbate risk of colorectal cancer development in people with previous X-ray exposure. Patients should be carefully followed up especially with bowel inflammation.

Acknowledgements

This work was supported in part by a Grant-in-Aid for the Third-term Comprehensive 10-year Strategy for Cancer Control, a Grant-in-Aid for Cancer Research from the Ministry of Health, Labour and Welfare, Japan, and a Grant-in-Aid from Central Research Institute of Electric Power Industry (CRIEPI), Japan.

References

Balkwill F, Mantovani A (2001). Inflammation and cancer: back to Virchow? *Lancet*, **357**, 539-45.

Bolla M, Verry C, Long JA (2013). High-risk prostate cancer: combination of high-dose, high-precision radiotherapy and androgen deprivation therapy. *Curr Opin Urol*, **23**, 349-54.

Brown AP, Neeley ES, Werner T, et al (2010). A population-based study of subsequent primary malignancies after endometrial cancer: genetic, environmental, and treatment-related associations. *Int J Radiat Oncol Biol Phys*, **78**, 127-35.

Chang ML, Hou JK (2011). Cancer risk related to gastrointestinal diagnostic radiation exposure. *Curr Gastroenterol Rep*, **13**, 449-57.

Choi KH, Ha M, Lee WJ, et al (2013). Cancer risk in diagnostic radiation workers in Korea from 1996-2002. *Int J Environ Res Public Health*, **10**, 314-27.

Kinzler KW, Vogelstein B (1996). Lessons from hereditary colorectal cancer. *Cell*, **87**, 159-70.

Kohno H, Suzuki R, Sugie S, et al (2005). Beta-Catenin mutations in a mouse model of inflammation-related colon carcinogenesis induced by 1,2-dimethylhydrazine and dextran sodium sulfate. *Cancer Sci*, **96**, 69-76.

Luongo C, Dove WF (1996). Somatic genetic events linked to the Apc locus in intestinal adenomas of the Min mouse. *Genes Chromosomes Cancer*, **17**, 194-8.

Moser AR, Pitot HC, Dove WF (1990). A dominant mutation that predisposes to multiple intestinal neoplasia in the mouse. *Science*, **247**, 322-4.

Munkholm P (2003). Review article: the incidence and prevalence of colorectal cancer in inflammatory bowel disease. *Aliment Pharmacol Ther*, **18**, 1-5.

Nottage K, McFarlane J, Krasin MJ, et al (2012). Secondary colorectal carcinoma after childhood cancer. *J Clin Oncol*, **30**, 2552-8.

Ohshima H, Tatemichi M, Sawa T (2003). Chemical basis of inflammation-induced carcinogenesis. *Arch Biochem Biophys*, **417**, 3-11.

Okamoto M, Yonekawa H (2005). Intestinal tumorigenesis in Min mice is enhanced by X-irradiation in an age-dependent manner. *J Radiat Res*, **46**, 83-91.

Okayasu I, Hatakeyama S, Yamada M, et al (1990). A novel method in the induction of reliable experimental acute and chronic ulcerative colitis in mice. *Gastroenterology*, **98**, 694-702.

Ozasa K, Shimizu Y, Suyama A, et al (2012). Studies of the mortality of atomic bomb survivors, Report 14, 1950-2003: an overview of cancer and noncancer diseases. *Radiat Res*, **177**, 229-43.

Paulsen JE, Steffensen IL, Namork E, et al (2003). Age-dependent susceptibility to azoxymethane-induced and spontaneous tumorigenesis in the Min/+ mouse. *Anticancer Res*, **23**, 259-65.

Powell SM, Petersen GM, Krush AJ, et al (1993). Molecular diagnosis of familial adenomatous polyposis. *N Engl J Med*, **329**, 1982-7.

Rydberg B (1996) Clusters of DNA damage induced by ionizing radiation: formation of short DNA fragments. II. Experimental detection. *Radiat Res*, **145**, 200-9.

Samartzis D, Nishi N, Cologne J, et al (2013). Ionizing radiation exposure and the development of soft-tissue sarcomas in atomic-bomb survivors. *J Bone Joint Surg Am*, **95**, 222-9.

Shoemaker AR, Moser AR, Dove WF (1995) *N*-ethyl-*N*-nitrosourea treatment of multiple intestinal neoplasia (Min) mice: age-related effects on the formation of intestinal adenomas, cystic crypts, and epidermoid cysts. *Cancer Res*, **55**, 4479-85.

Steffensen IL, Paulsen JE, Eide TJ, et al (1997). 2-Amino-1-methyl-6-phenylimidazo[4,5-b]pyridine increases the numbers of tumors, cystic crypts and aberrant crypt foci in multiple intestinal neoplasia mice. *Carcinogenesis*, **18**, 1049-54.

Su LK, Kinzler KW, Vogelstein B, et al (1992). Multiple

intestinal neoplasia caused by a mutation in the murine homolog of the APC gene. *Science*, **256**, 668-70.

Tamai O, Nozato E, Miyazato H, et al (1999). Radiation-associated rectal cancer: report of four cases. *Dig Surg*, **16**, 238-43.

Tanaka T, Kohno H, Suzuki R, et al (2006). Dextran sodium sulfate strongly promotes colorectal carcinogenesis in Apc(Min/+) mice: inflammatory stimuli by dextran sodium sulfate results in development of multiple colonic neoplasms. *Int J Cancer*, **118**, 25-34.

Tanaka T, Kohno H, Suzuki R, et al (2003). A novel inflammation-related mouse colon carcinogenesis model induced by azoxymethane and dextran sodium sulfate. *Cancer Sci*, **94**, 965-73.

Tanaka T, Suzuki R, Kohno H, et al (2005). Colonic adenocarcinomas rapidly induced by the combined treatment with 2-amino-1-methyl-6-phenylimidazo[4,5-b]pyridine and dextran sodium sulfate in male ICR mice possess beta-catenin gene mutations and increases immunoreactivity for beta-catenin, cyclooxygenase-2 and inducible nitric oxide synthase. *Carcinogenesis*, **26**, 229-38.

Toyoda et al. BMC Gastroenterology 2013, 13:122
http://www.biomedcentral.com/1471-230X/13/122

BMC Gastroenterology

RESEARCH ARTICLE Open Access

Gene expression analysis of a *Helicobacter pylori*-infected and high-salt diet-treated mouse gastric tumor model: identification of CD177 as a novel prognostic factor in patients with gastric cancer

Takeshi Toyoda[1,2†], Tetsuya Tsukamoto[3*†], Masami Yamamoto[4], Hisayo Ban[2], Noriko Saito[2], Shinji Takasu[1], Liang Shi[5], Ayumi Saito[6], Seiji Ito[7], Yoshitaka Yamamura[7], Akiyoshi Nishikawa[8], Kumiko Ogawa[1], Takuji Tanaka[9] and Masae Tatematsu[10]

Abstract

Background: *Helicobacter pylori* (*H. pylori*) infection and excessive salt intake are known as important risk factors for stomach cancer in humans. However, interactions of these two factors with gene expression profiles during gastric carcinogenesis remain unclear. In the present study, we investigated the global gene expression associated with stomach carcinogenesis and prognosis of human gastric cancer using a mouse model.

Methods: To find candidate genes involved in stomach carcinogenesis, we firstly constructed a carcinogen-induced mouse gastric tumor model combined with *H. pylori* infection and high-salt diet. C57BL/6J mice were given *N*-methyl-*N*-nitrosourea in their drinking water and sacrificed after 40 weeks. Animals of a combination group were inoculated with *H. pylori* and fed a high-salt diet. Gene expression profiles in glandular stomach of the mice were investigated by oligonucleotide microarray. Second, we examined an availability of the candidate gene as prognostic factor for human patients. Immunohistochemical analysis of CD177, one of the up-regulated genes, was performed in human advanced gastric cancer specimens to evaluate the association with prognosis.

Results: The multiplicity of gastric tumor in carcinogen-treated mice was significantly increased by combination of *H. pylori* infection and high-salt diet. In the microarray analysis, 35 and 31 more than two-fold up-regulated and down-regulated genes, respectively, were detected in the *H. pylori*-infection and high-salt diet combined group compared with the other groups. Quantitative RT-PCR confirmed significant over-expression of two candidate genes including *Cd177* and *Reg3g*. On immunohistochemical analysis of CD177 in human advanced gastric cancer specimens, over-expression was evident in 33 (60.0%) of 55 cases, significantly correlating with a favorable prognosis ($P = 0.0294$). Multivariate analysis including clinicopathological factors as covariates revealed high expression of CD177 to be an independent prognostic factor for overall survival.

(Continued on next page)

* Correspondence: ttsukamt@fujita-hu.ac.jp
†Equal contributors
[3]Department of Pathology, Fujita Health University School of Medicine, Toyoake, Japan
Full list of author information is available at the end of the article

(Continued from previous page)

Conclusions: These results suggest that our mouse model combined with *H. pylori* infection and high-salt diet is useful for gene expression profiling in gastric carcinogenesis, providing evidence that CD177 is a novel prognostic factor for stomach cancer. This is the first report showing a prognostic correlation between CD177 expression and solid tumor behavior.

Keywords: Cd177, Gastric cancer, *Helicobacter pylori*, Microarray, Salt

Background

Stomach cancer is the fourth most common cancer and second leading cause of cancer-related death worldwide [1]. *Helicobacter pylori* (*H. pylori*) is now recognized as a major risk factor for chronic gastritis and stomach cancer development [2]. In addition, environmental and host factors have also been shown to influence gastric carcinogenesis, and salt (sodium chloride, NaCl) and salty food are of particular importance, based on evidence from a number of epidemiological and experimental studies [3-6]. Thus, combined exposure to *H. pylori* infection and excessive salt intake appears to be very important for the development and progression of gastric tumors, although the detailed mechanisms, especially in terms of gene expression profiles, remain to be clarified.

High throughput microarray technology provides a powerful tool for comprehensive gene analysis, already applied to assess gene expression patterns in both human samples and animal models of gastric disorders [7-16]. Although many researchers have focused on gene expression in *H. pylori*-treated gastric cell lines [17-19], results in cell culture do not necessarily correlate with expression of specific genes in the *in vivo* microenvironment featuring host immune responses and stromal-epithelial interactions in cancers. Carcinogen-treated Mongolian gerbils have been used as a useful animal model of *H. pylori*-associated gastric carcinogenesis [20-24], and we previously reported that a synergistic interaction between *H. pylori* infection and high-salt intake accelerates chronic inflammation and tumor development in the stomachs of these animals [25,26]. Unfortunately, there is little information available for the gerbil genome, hampering genetic and molecular analysis. Therefore, attention has focused on mouse models [12,13], and establishment of a mouse model for stomach cancer featuring salt and *H. pylori* exposure is needed for investigations targeting genes involved in gastric carcinogenesis.

Previous microarray studies using rodent models did not distinguish and characterize expression profiles based on the interaction of *H. pylori* infection and salt intake. In the present study, we examined gene expression in the gastric mucosa in a *H. pylori*-infected and high-salt diet-treated mouse gastric tumor model by oligonucleotide microarray and found two candidate up-regulated genes including *Cd177* and *Reg3g*. We also investigated the expression of CD177 in human advanced gastric cancers by immunohistochemistry, and obtained evidence as a potential prognostic factor for stomach carcinogenesis.

Methods

Inoculation with *H. pylori*

H. pylori was prepared by the same method as described previously [27,28]. Briefly, *H. pylori* (Sydney strain 1) was inoculated on Brucella agar plates (Becton Dickinson, Cockeysville, MD, USA) containing 7% (v/v) heat-inactivated fetal bovine serum (FBS) and incubated at 37°C under microaerophilic conditions at high humidity for 2 days. Then, bacteria grown on the plates were introduced into Brucella broth (Becton Dickinson) supplemented with 7% (v/v) FBS and incubated under the same conditions for 24-h. After 24-h fasting, animals were intra-gastrically inoculated *H. pylori* (1.0×10^8 colony-forming units). Before inoculation, the broth cultures of *H. pylori* were checked under a phase-contrast microscope for bacterial shape and mobility.

Animals and experimental protocol

Fifty-six specific pathogen-free male, 5- or 6-week-old C57BL/6J mice (CLEA Japan, Tokyo, Japan) were used in this study. All animals were housed in plastic cages on hardwood-chip bedding in an air-conditioned biohazard room with a 12-h light/12-h dark cycle, and allowed free access to food and water throughout. The experimental design was approved by the Animal Care Committee of the Aichi Cancer Center Research Institute, and the animals were cared for in accordance with institutional guidelines as well as the Guidelines for Proper Conduct of Animal Experiments (Science Council of Japan, June 1st, 2006).

The experimental design is illustrated in Figure 1A. The mice were divided into 4 groups (Groups A-D); 21, 5, 15, and 15 mice were assigned to A, B, C, and D groups, respectively, at the commencement of the experiment. Animals of Groups B and D were inoculated with *H. pylori* intra-gastrically on alternate weeks (total 7 times), while mice of the other groups were inoculated with Brucella broth alone. All mice were given *N*-methyl-*N*-nitrosourea (MNU, Sigma Chemical, St Louis, MO, USA) in their drinking water at the concentration of 120 ppm on alternate weeks (total exposure was 5 weeks). For this purpose

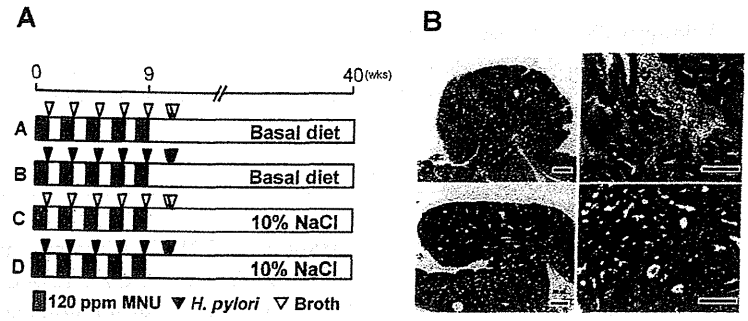

Figure 1 Experimental design and histopathological findings. A: Experimental design. Five- to six-week-old male C57BL/6J mice were inoculated with *H. pylori* SS1 strain (Groups B and D) or Brucella broth (Groups A and C). All animals were administered 120 ppm MNU in their drinking water on alternate weeks (total exposure, 5 weeks). Mice of Groups C and D were given basal diet (CE-2) containing 10% NaCl. **B**: Histopathological findings for MNU-induced mice gastric tumors. (a and b) Gastric adenoma in the pyloric region of an MNU-treated and *H. pylori*-infected mouse (Group B). (c and d) Gastric adenocarcinoma observed in Group B. Note the high cell density and cellular and structural atypia. Bar = 200 (a and c) or 100 μm (b and d).

MNU was freshly dissolved in distilled water three times per week. Mice of Groups C and D received CE-2 diets (basal sodium content of 0.36%; CLEA Japan) containing 10% NaCl. During the exposure period, one animal of Group B, one of Group C and six of Group D died or became moribund and they were excluded from the experiment. At 40 weeks, the remained animals were subjected to deep anesthesia and laparotomy with excision of the stomach.

Histological evaluation

For histological examination, the stomachs were fixed in 10% neutral-buffered formalin for 24-h, sliced along the longitudinal axis into strips of equal width, and embedded in paraffin. Four-μm thick sections were prepared and stained with hematoxylin and eosin (H&E) for histological observation. Tumors were classified into adenoma and adenocarcinoma based on cellular and morphological atypia and invasive growth to submucosa as we reported previously [21].

RNA preparation and oligonucleotide microarray analysis

Total RNA was extracted from the whole gastric mucosa including both tumor and peripheral tissue using an RNeasy Plus Mini Kit (Qiagen, Hilden, Germany) and its quality checked with a microchip electrophoresis system (i-chip SV1210; Hitachi Chemical, Tokyo, Japan). High-quality samples were selected, and pooled for each group to avoid individual difference for oligonucleotide microarray assessment (Group A, n = 3; B, n = 4; C, n = 6; D, n = 7). The CodeLink Mouse Whole Genome Bioarray (Applied Microarrays, Tempe, AZ, USA) containing 35,587 probe sets per chip was used to analyze gene expression profiles. Hybridization, processing, and scanning were performed by Filgen, Inc. (Nagoya, Japan), scan data images being analyzed using a software package (Microarray Data Analysis Tool, Filgen). Complete-linkage hierarchical clustering was also examined on the four groups using a qualified probe subset (Filgen).

Quantitative real-time RT-PCR of expression profiles in mice stomach

Relative quantitative real-time RT-PCR was performed using a StepOne Real-Time PCR System (Applied Biosystems, Foster City, CA, USA) with the mouse-specific glyceraldehyde-3-phosphate dehydrogenase (*Gapdh*) gene as an internal control. After DNase treatment, first strand cDNAs were synthesized from total RNA using a SuperScript VILO cDNA Synthesis Kit (Invitrogen, Carlsbad, CA, USA). The PCR was accomplished basically following the manufacturer's instructions using a QuantiTect SYBR Green PCR Kit (Qiagen). The primer sequences for each gene are listed in Table 1. Specificity of the PCR reactions was confirmed using a melt curve program provided with the StepOne software and electrophoresis of the PCR samples in 3% agarose gels. The expression levels of mRNAs were normalized to the mRNA level of *Gapdh* and compared with the control mice (Group A) by the ΔΔCT method.

Patients and tumor specimens

A total of 55 cases of primary advanced gastric cancer, surgically resected at Aichi Cancer Center Hospital (Nagoya, Japan) between 1995 and 2002, were investigated after obtaining informed consent. The study was approved by the ethics committee of Aichi Cancer Center. The patients were all male and the mean age and median follow-up period were 58.6 ± 10.2 years and 83 weeks, respectively. None had received preoperative chemotherapy or radiotherapy. Carcinomas with adjacent mucosa tissue were fixed and embedded in paraffin, and sectioned for staining

Table 1 Primer sequences for relative quantitative real-time RT-PCR

Gene	Sequences	Product length	Accession no.
Gapdh	5′-AACGGATTTGGCCGTATTG-3′	140	NM_008084
	5′-TTGCCGTGAGTGGAGTCATA-3′		
Cd177	5′-AGGGGTGCCACTCACTGTTA-3′	128	NM_026862
	5′-CCGATTGTTTTGGAGTCACC-3		
Reg3g	5′-GTATGGATTGGGCTCCATGA-3′	106	NM_011260
	5′-GATTCGTCTCCCAGTTGATG-3′		
Muc13	5′-CCTAATCCCTACGCAAACCA-3′	124	NM_010739
	5′-TCTGCCCATTTCTCCTTGTC-3′		

Gapdh glyceraldehyde-3-phosphate dehydrogenase, *Reg3g* regenerating islet-derived protein 3 gamma, *Muc13* mucin 13.

with H&E. Classification of tumor staging and diagnosis of advanced cases were made according to the Japanese Classification of Gastric Carcinomas [29]. The cancers had invaded the muscularis propria (T2 for TNM classification), the subserosa (T3), or the serosa and the peritoneal cavity (T4a), sometimes involving adjacent organs (T4b).

Immunohistochemistry using human gastric cancer tissue

We examined expression of CD177, for which a commercial primary antibody was available, in human gastric cancer tissues by immunohistochemistry. After inhibition of endogenous peroxidase activity by immersion in 3% hydrogen peroxide/methanol solution, antigen retrieval was carried out with 10 mM citrate buffer (pH 6.0) in a microwave oven for 10 min at 98°C. Then, sections were incubated with a mouse monoclonal anti-CD177 antibody (clone 4C4, diluted 1:100, Abnova, Taipei, Taiwan). Staining for CD177 was performed using a Vectastain Elite ABC Kit (Vector Laboratories, Burlingame, CA, USA) and binding visualized with 0.05% 3,3′-diaminobenzidine. The results of CD177 immunostaining in neoplastic cells were classified into four degrees; grade 0 (none, 0-10% of positive cells), grade 1 (weak, 10-30%), grade 2 (moderate, 30-60%), and grade 3 (strong, over 60%) based on proportion of stained cells, and cases showing moderate to strong staining were considered as positive.

Statistical analysis

The Chi-square test with Bonferroni correction was used to assess incidences of gastric tumor. Quantitative values including multiplicity of tumor and relative expression of mRNA were represented as means ± SD or SE, and differences between means were statistically analyzed by ANOVA or the Kruskal-Wallis test followed by the Tukey test for multiple comparisons. Overall survival was estimated using the Kaplan-Meier method and the log-rank test for comparisons. Correlations between CD177 expression and clinicopathological factors were analyzed by ANOVA or Chi-square test. Multivariate analysis was performed to examine whether CD177 over-expression was an independent prognostic factor using the Cox proportional-hazards regression model. P values of < 0.05 were considered to be statistically significant.

Results

Incidences and multiplicities of gastric tumors

The effective number of mice and the observed incidences and multiplicities of gastric tumors are summarized in Table 2. Tumors developed in the gastric mucosa of all MNU-treated groups (Groups A-D) (Figure 1B). In high-salt diet-treated groups (Groups C and D), the incidence of gastric tumor in Group D (*H. pylori*-infected; 100%) was significantly higher than that in Group C (non-infected; 50.0%) ($P < 0.05$). In basal diet groups (Groups A

Table 2 Incidence and multiplicity of gastric tumors in MNU-treated mice

Group	Effective number	Treatment	Incidence (%)			Multiplicity (no. of tumor/mouse)		
			Adenoma	Carcinoma	Total tumor	Adenoma	Carcinoma	Total tumor
A	21	MNU	3(14.3)	13(61.9)	13(61.9)	0.1 ± 0.4[a]	0.8 ± 0.7	0.9 ± 0.8
B	4	MNU + *H. pylori*	4(100)[b]	4(100)	4(100)	1.5 ± 0.6	1.8 ± 1.0	3.3 ± 1.0[c]
C	14	MNU + 10% NaCl	2(14.3)	6(42.9)	7(50.0)	0.2 ± 0.6	0.8 ± 1.0	1.0 ± 1.2
D	9	MNU + *H. pylori* + 10% NaCl	4(44.4)	8(88.8)	9(100)[d]	0.4 ± 0.5[e]	2.1 ±1.4[d]	2.6 ± 1.1[d]

Values for multiplicity are expressed as means ± SD. Incidences were generally assessed by Chi-square test, followed by pairwise analysis with Bonferroni correction. Multiplicities were generally analyzed by ANOVA, followed by the Tukey test for multiple comparison. [a]$P < 0.01$ *vs.* Group B, [b]$P < 0.01$ *vs.* Group A, [c]$P < 0.05$ *vs.* Group A, [d]$P < 0.05$ *vs.* Group C, [e]$P < 0.05$ *vs.* Group B.

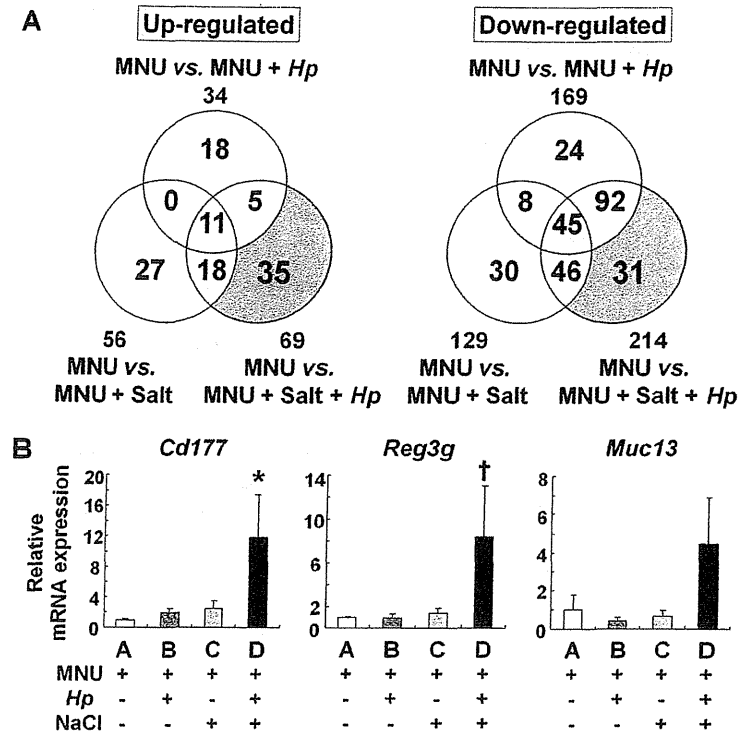

Figure 2 Global gene analysis in the glandular stomach of MNU-treated mice using oligonucleotide microarray. A: Number of genes up- or down-regulated more than two-fold in the stomach of MNU-treated mice. In Venn's diagram, the circles indicate up- (left) or down-regulated (right) genes in the stomach of MNU-treated mice with *H. pylori* infection, high-salt diet or their combination. The shaded area represents the up- or down-regulated genes more than two-fold only by the combination. **B**: Quantitative real-time RT-PCR analysis of three selected up-regulated genes (*Cd177*, *Reg3g*, and *Muc13*) in the stomachs of MNU-treated mice. Expression levels of the genes in each sample were normalized by *Gapdh* as internal control using ΔΔCT method. Relative expression levels were represented as the X-fold change relative to Group A (fixed as 1.0). Statistical analysis was performed by the Kruskal-Wallis test for general analysis and Tukey test for multiple comparison. Bars, SE; *, $P < 0.01$ *vs.* Group A and < 0.05 *vs.* Group C; †, $P < 0.01$ *vs.* Group C.

and B), the incidence was also increased by *H. pylori*-infection (Group A, 61.9% and Group B, 100%), albeit without statistical significance. The multiplicities of total tumors in both *H. pylori*-infected groups (Group B, 3.3 ± 1.0 tumors/mouse and Group D, 2.6 ± 1.1) were markedly higher than those in non-infected groups (Group A, 0.9 ± 0.8 and Group C, 1.0 ± 1.2) ($P < 0.05$). The multiplicity of gastric adenocarcinoma in Group D (2.1 ± 1.4) was slightly higher than that in Group B (1.8 ± 1.0) and significantly increased over the Group C value (0.8 ± 1.0) ($P < 0.05$). In contrast, the multiplicities of adenomas in Groups A and D (0.1 ± 0.4 and 0.4 ± 0.5, respectively) were significantly lower than in Group B (1.5 ± 0.6) ($P < 0.05$ and 0.01).

Gene expression profiling in the glandular stomachs by oligonucleotide microarray

With oligonucleotide microarrays, compared with the non-infected and basal diet-treated group (Group A), 34 genes were up-regulated and 169 were down-regulated more than two-fold in *H. pylori*-infected mice (Group B), 56 up-regulated and 129 down-regulated in high-salt diet-treated mice (Group C), and 69 up-regulated and 214 down-regulated in the combined group (Group D) (Figure 2A). Taken together, as shown in Table 3, we found that 35 genes were up-regulated and 31 genes were down-regulated more than two-fold only by the combination of *H. pylori* infection and high-salt diet. In addition, hierarchical clustering analysis was performed on the four groups with a total of 303 qualified probes using the complete-linkage clustering algorithm (Figure 3). Thirty-one probes including *Cd177*, *Reg3g* and *Muc13* were confirmed to be within a cluster of probes up-regulated only in Group D. Subsequent analysis in the present study was focused on these genes, because it was considered that the genes in which expression was altered only in the combined group might be associated with gastric carcinogenesis and progression in humans.

The entire results of this microarray analysis have been submitted and are readily retrievable from the

Table 3 Regulated genes by combination of *H. pylori* infection and high-salt diet in mouse gastric mucosa

Accession no.	Symbol	Genes/proteins	Fold changes
Up-regulated genes			
XM_357640	Igk-V8	Immunoglobulin kappa chain variable 8 (V8)	14.4
XM_001472541	Ighg	Immunoglobulin heavy chain (gamma polypeptide)	9.2
NM_026862	Cd177	CD177 antigen	7.3
NM_011260	Reg3g	Regenerating islet-derived 3 gamma	6.1
NM_023137	Ubd	Ubiquitin D	4.3
XM_144817	Igk-V34	Immunoglobulin kappa chain variable 34 (V34)	4.1
NM_007675	Ceacam10	Carcinoembryonic antigen-related cell adhesion molecule 10	3.7
NM_183322	Khdc1a	KH domain containing 1A	3.3
NM_011475	Sprr2i	Small proline-rich protein 2I	3.2
NM_175165	Tprg	Transformation related protein 63 regulated	3.2
NM_175406	Atp6v0d2	ATPase, H+ transporting, lysosomal V0 subunit D2	3.0
NM_009703	Araf	v-raf murine sarcoma 3611 viral oncogene homolog	2.6
NM_026822	Lce1b	Late cornified envelope 1B	2.5
NM_016958	Krt14	Keratin 14	2.5
NM_212487	Krt78	Keratin 78	2.4
NM_009807	Casp1	Caspase 1	2.4
NM_146037	Kcnk13	Potassium channel, subfamily K, member 13	2.4
NM_019450	Il1f6	Interleukin 1 family, member 6	2.3
NM_008827	Pgf	Placental growth factor	2.3
XM_893506	Klk12	Kallikrein related-peptidase 12	2.3
NM_016887	Cldn7	Claudin 7	2.3
NM_029360	Tm4sf5	Transmembrane 4 superfamily member 5	2.2
NM_172301	Ccnb1	Cyclin B1	2.2
NM_010739	Muc13	Mucin 13, epithelial transmembrane	2.2
NM_011165	Prl4a1	Prolactin family 4, subfamily a, member 1	2.2
NM_010162	Ext1	Exostoses (multiple) 1	2.2
NM_011704	Vnn1	Vanin 1	2.1
NM_011082	Pigr	Polymeric immunoglobulin receptor	2.1
NM_007769	Dmbt1	Deleted in malignant brain tumors 1	2.1
NM_022984	Retn	Resistin	2.1
NM_173037	Tmco 7	Transmembrane and coiled-coil domain 7	2.1
NM_009100	Rptn	Repetin	2.1
NM_007630	Ccnb2	Cyclin B2	2.1
NM_001081060	Slc9a3	Solute carrier family 9 (sodium/hydrogen exchanger), member 3	2.0
NM_146588	Olfr1030	Olfactory receptor 1030	2.0
Down-regulated genes			
NM_008753	Oaz1	Ornithine decarboxylase antizyme 1	0.31
NM_027126	Hfe2	Hemochromatosis type 2 (juvenile) (human homolog)	0.33
NM_053206	Magee2	Melanoma antigen, family E, 2	0.33
NM_010924	Nnmt	Nicotinamide N-methyltransferase	0.41
NM_026260	Tctn3	Tectonic family member 3	0.41
NM_181039	Lphn1	Latrophilin 1	0.43
NM_008312	Htr2c	5-hydroxytryptamine (serotonin) receptor 2C	0.43

Table 3 Regulated genes by combination of *H. pylori* infection and high-salt diet in mouse gastric mucosa *(Continued)*

NM_146667	Olfr740	Olfactory receptor 740	0.44
NM_007550	Blm	Bloom syndrome homolog (human)	0.44
NM_011243	Rarb	Retinoic acid receptor, beta	0.44
NM_184052	Igf1	Insulin-like growth factor 1	0.45
NM_013893	Reg3d	Regenerating islet-derived 3 delta	0.46
NM_008645	Mug1	Murinoglobulin 1	0.46
NM_029550	Keg1	Kidney expressed gene 1	0.46
NM_019388	Cd86	CD86 antigen	0.46
NM_011316	Saa4	Serum amyloid A 4	0.47
NM_007811	Cyp26a1	Cytochrome P450, family 26, subfamily a, polypeptide 1	0.47
NM_011538	Tbx6	T-box 6	0.48
NM_011086	Pip5k3	Phosphatidylinositol-3-phospate/phosphatidylinositol 5-kinase, type III	0.48
NM_133723	Asph	Aspartate-beta-hydroxylase	0.48
NM_001081390	Palld	Palladin, cytoskeletal associated protein	0.48
NM_007858	Diap1	Diaphanous homolog 1 (Drosophila)	0.48
NM_053271	Rims2	Regulating synaptic membrane exocytosis 2	0.48
NM_153163	Cadps2	Ca2+–dependent activator protein for secretion 2	0.49
NM_007541	Bglap1	Bone gamma carboxyglutamate protein 1	0.49
NM_031871	Ghdc	GH3 domain containing	0.49
NM_025545	Aptx	Aprataxin	0.49
NM_177322	Agtr1a	Angiotensin II receptor, type 1a	0.49
NM_026872	Ubap2	Ubiquitin-associated protein 2	0.49
NM_028045	Erv3	Endogenous retroviral sequence 3	0.49
NM_011641	Trp63	Transformation related protein 63	0.49

public database NCBI Gene Expression Omnibus (GEO) with the accession number GSE29444 (sample number: GSM728857-60).

Quantitative real-time RT-PCR analysis of gene expression profiles in MNU-treated mouse stomachs

Relative quantitative real-time RT-PCR analysis of three selected up-regulated genes (*Cd177*, *Reg3g*, and *Muc13*) in *H. pylori*-infected and high-salt diet-treated mice confirmed increased expression of *Cd177* and *Reg3g*, as shown in Figure 2B, with significant differences. Although expression level of *Muc13* in Group D was higher than all other groups, there was no statistical significance among them ($P = 0.0712$ *vs.* Group C).

Immunohistochemical expression of CD177 in human advanced gastric cancers and correlation with clinicopathological factors

On immunohistochemical analysis of human gastric cancer tissues, CD177 was observed not only in the membranes and cytoplasms of infiltrated neutrophils, but also in gastric cancer cells of both well- and poorly-differentiated adenocarcinomas (Figure 4A). Cancer cells of signet-ring cell type (2 cases) were negative for CD177. Among 55 gastric cancer cases, moderate to strong expression of CD177 was observed in 33 (60.0%) (Table 4).

The follow-up period of the patients ranged from 9 to 606 weeks (median = 83 weeks). Five-year survival rates for CD177-positive and negative were 39.4% and 18.2%, respectively. From the Kaplan-Meier survival curve analysis, CD177-positive expression was associated with better overall survival ($P = 0.0294$, log-rank test) (Figure 4B). There was no statistically significant correlation of CD177 expression with age, histological classification, depth of invasion, and lymph node metastasis (Table 4).

Multivariate analysis for overall survival of human gastric cancer cases

Using the Cox proportional hazards model, multivariate analysis of clinicopathological variables, including the patient age, tumor histological classification, invasion depth, lymph node metastasis, and CD177 expression (Table 5), revealed the last to be an independent factor for overall survival ($P = 0.0323$). Patient age and low

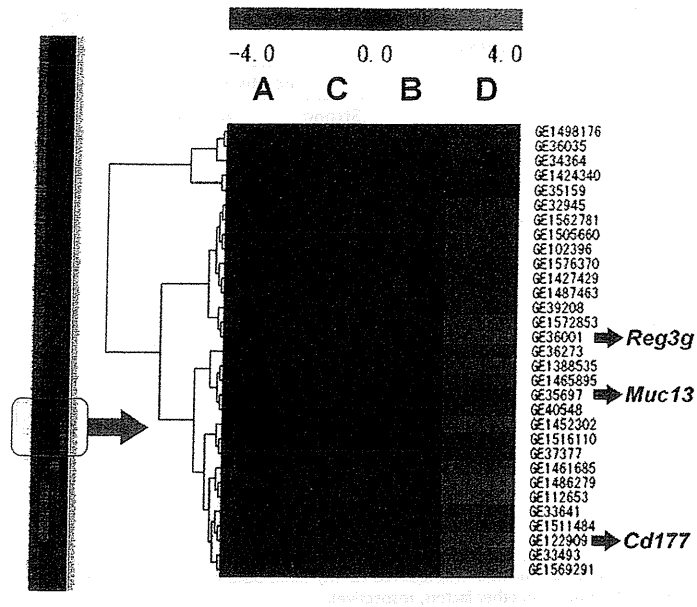

Figure 3 Hierarchical clustering analysis of four experimental groups of MNU-treated mice. Expression data from 303 qualified probes (left). The four experimental groups were classified into two clusters (Groups A/C) and (Groups B/D) based on similarities in expression patterns. Each row represents a probe and each column represents a experimental group (Groups A-D). As shown in the color bar, green indicates up-regulation; red indicates down-regulation; and black indicates no change. Thirty-one probes constituted a cluster of probes up-regulated only in Group D (right).

differentiation of adenocarcinoma were also associated with poor overall survival (P = 0.0439 and 0.0017, respectively). Tumor invasion depth and lymph node metastasis were not independent factors of gastric cancer cases in the present study ($P > 0.05$).

Discussion

In the present study, we demonstrated that the mouse model combined with *H. pylori* infection and high-salt diet is a useful tool to investigate the detailed mechanisms both of development and progression of gastric

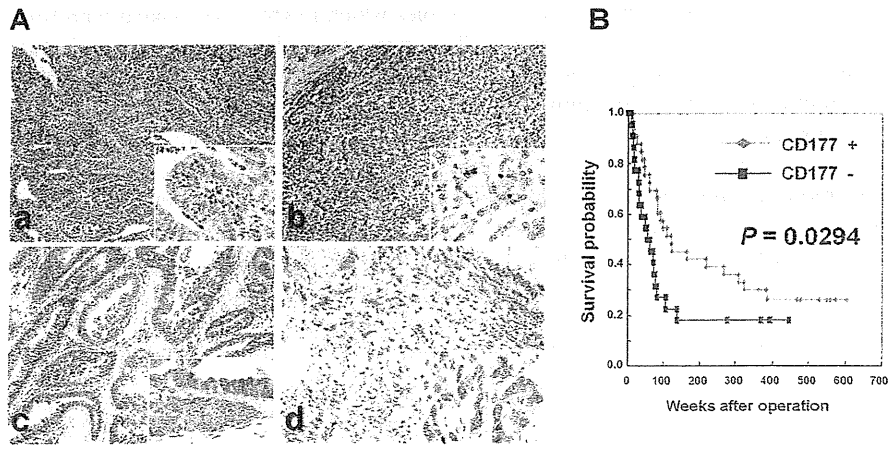

Figure 4 Immunohistochemistry for CD177 in human advanced gastric cancer and correlation with overall survival rate. A: Immunohistochemical analysis of CD177 expression in human gastric cancer tissue. (a and b) Negative staining (none to weak) for CD177 in a gastric adenocarcinoma. CD177 expression is present only in infiltrating neutrophils while neoplastic cells of well-differentiated (a) or poorly-differentiated (b) carcinoma are negative. Original magnification, ×100 (inset, ×400). (c and d) Note positive (moderate to strong) expression for CD177 in well-differentiated (c) or poorly-differentiated (d) gastric cancer cells. Original magnification, ×100 (inset, ×400). B: Comparison of Kaplan-Meier cumulative survival curves for CD177 negative and positive gastric cancer cases.